VWR®
We Enable Science

Volume 3, Issue 2

VWR bioMarke™

CONTENTS

Rapidly Obtain High Yields of Soluble Protein with Vmax™ Express Electrocompetent Cells

SGI-DNA
A Synthetic Genomics, Inc. Company

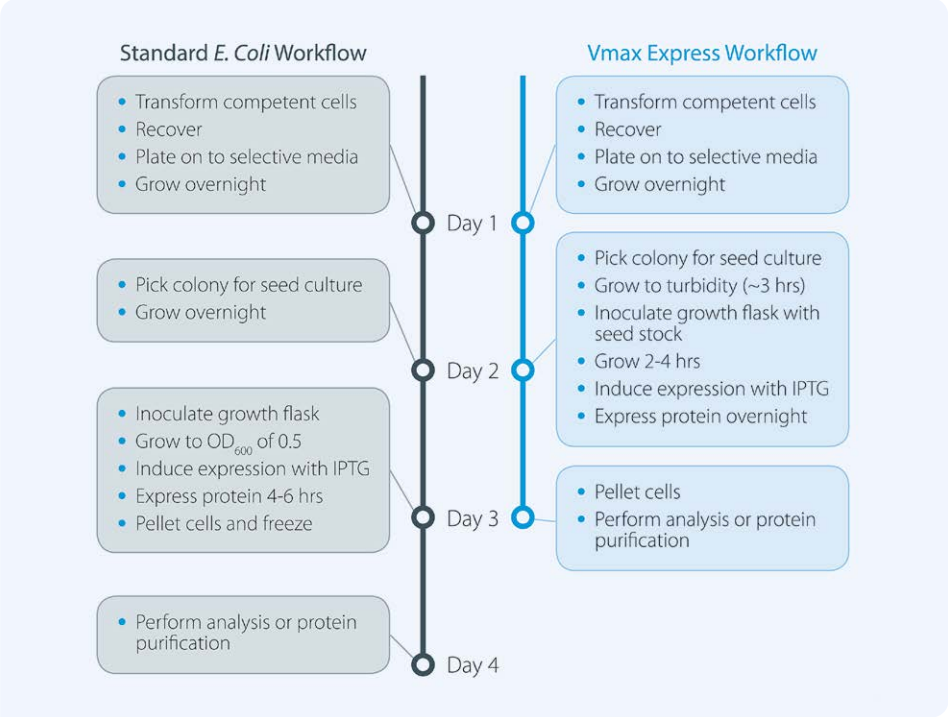

Figure 1. Vmax™ Express generates recombinant proteins one day faster than *E. coli.*

For recombinant protein expression, *E. coli* has been the longstanding protein expression workhorse. Pioneering studies elucidating DNA replication, transcription, and translation[1–4] performed in *E. coli* resulted in the routine use of *E. coli* for molecular biology workflows. Although *E. coli* strains such as BL21 have been modified and adapted for recombinant protein expression, challenges such as low expression levels and the expression of proteins as insoluble inclusion bodies frequently occur. Attempts to overcome these *E. coli* protein expression problems using protocol modifications, such as changes to growth conditions, are often unsuccessful.

Recognizing that the routine use of *E. coli* is largely due to historical reasons, and postulating that a rationally-designed system could avoid some of the *E. coli* protein expression issues, scientists at Synthetic Genomics Inc. (SGI) set out to design and engineer an alternative molecular biology host system. Specifically, the team sought to identify a more effective, fast-growing host to accelerate and improve molecular biology workflows. The search for this microorganism led to a report from the early 1960s on the bacterium *Vibrio natriegens*[5], a non-pathogenic, gram-negative bacterium naturally found in salt marsh mud with a doubling time more than twice that of *E. coli.* Leveraging the genetic tools and methods developed during the construction of the first minimal synthetic cell[6], SGI and SGI-DNA research teams used *V. natriegens* to create a new protein expression host, Vmax Express.

Vmax Express Electrocompetent Cells are engineered to retain all of the benefits of traditional bacterial protein expression systems — low cost, ease-of-growth, and high compatibility with plasmids and antibiotics already in widespread use — while avoiding low expression and solubility issues. With a doubling time of about 14 minutes, Vmax Express is not only able to shorten protein expression workflows by one day (see Figure 1), but it is also able to produce greater amounts of biomass and generate more soluble protein than *E. coli.*

Vmax Express Generates Larger Amounts of Soluble Protein

To evaluate expression levels in Vmax™ Express, a Green Fluorescent Protein (GFP) expression plasmid was introduced into Vmax Express cells. Recombinant protein expression was induced with IPTG when cells reached an OD_{600} of 0.5 (Figure 2).

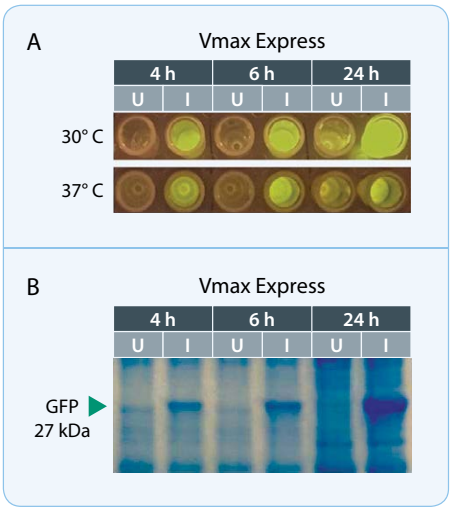

Figure 2. High levels of GFP expression in Vmax™ Express cells.

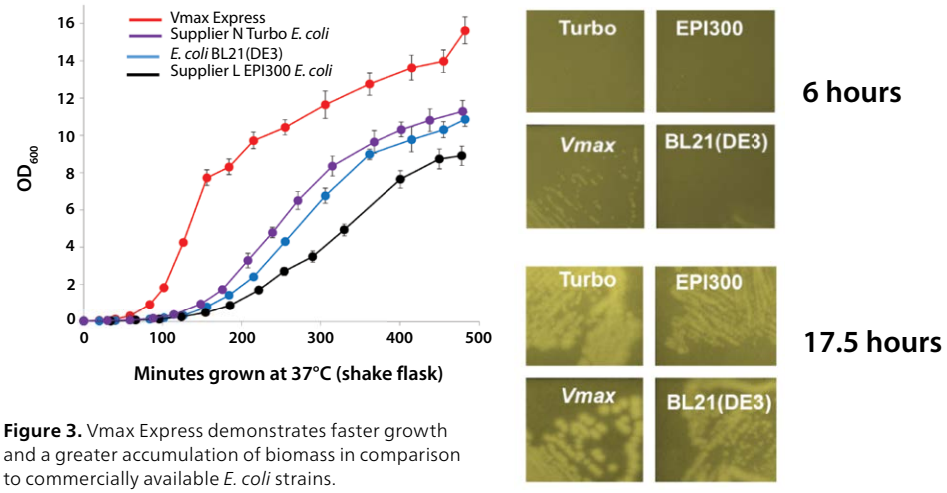

Figure 3. Vmax Express demonstrates faster growth and a greater accumulation of biomass in comparison to commercially available *E. coli* strains.

Except where indicated in figure 2, expression was performed at 30°C. At the time points indicated, samples of IPTG-induced (I) cells and uninduced (U) cells were analyzed. UV light was used to visualize active GFP in equal volumes of each cell lysate (Figure 2A). Detectable signal was observed in all induced samples. Lysates were examined by SDS-PAGE followed by Coomassie® Blue staining to visualize the amounts of expressed 27kDa GFP protein (Figure 2B). Vmax Express demonstrated a consistent increase in the amount of protein expressed in IPTG-induced cultures.

Vmax Express: Fastest Growth Rate and Greater Biomass

Vmax Express demonstrates faster growth and a greater accumulation of biomass relative to other commonly used expression systems. To compare Vmax Express with *E. coli* expression systems, overnight cultures of Vmax Express and several *E. coli* expression strains were inoculated to an OD^{600} of 0.03 in Brain Heart Infusion Broth + v2 salts at 37°C. At the times indicated in Figure 3A, the OD^{600} of each culture was determined. Significantly greater biomass in Vmax Express was evident after only 90 minutes of growth. After approximately 2.5 hours of growth, Vmax Express cells exhibited over 10 times the amount of biomass of all other strains tested. The greater amount of biomass evident in Vmax Express cultures continued for all subsequent times tested, including when cultures were harvested 8 hours post-inoculation. As shown in Figure 3B, Vmax Express also generated clearly visible colonies after 6 hours of growth on agar plates in contrast to *E. coli* strains that required an overnight incubation.

Vmax Express Demonstrates Improved Solubility

A common problem associated with *E. coli*-based expression systems is that proteins expressed by *E. coli* are often found in insoluble inclusion bodies. In contrast to *E. coli* BL21 strains, Vmax Express demonstrates improved solubility for a number of proteins. One example, the expression of uronate dehydrogenase, is shown in Figure 4. Following induction and incubation to allow for recombinant protein expression, cells were lysed and centrifuged to remove insoluble protein. Both the soluble and the insoluble pellet fractions were analyzed on an SDS-PAGE gel stained with Coomassie Blue. In *E. coli*, recombinant uronate dehydrogenase is found in the insoluble fraction. In contrast, with Vmax Express, recombinant uronate dehydrogenase is visible in both the insoluble and soluble fractions, with the majority of the protein found in the soluble fraction.

Vmax Express Outperforms *E. coli* BL21 for the Expression of a Variety of Proteins

To further evaluate protein expression in Vmax Express cells, SGI-DNA performed side-by-side Vmax Express and *E. coli* expression studies. Recombinant protein expression of the proteins listed in the following table was compared in *E. coli* BL21(DE3) cells and Vmax Express cells. Protein expression was induced using 1.0mM IPTG at an OD_{600} of 0.5. After induction, cells were incubated for 4 and 24 hours. BL21 cells and Vmax Express cells were grown at their optimum temperatures of 37ºC and 30ºC, respectively. Protein expression was evaluated relative to an uninduced sample using SDS-PAGE stained with Coomassie Blue. As shown in Table 1, superior expression was observed in Vmax Express cells for 5 out of 6 proteins analyzed.

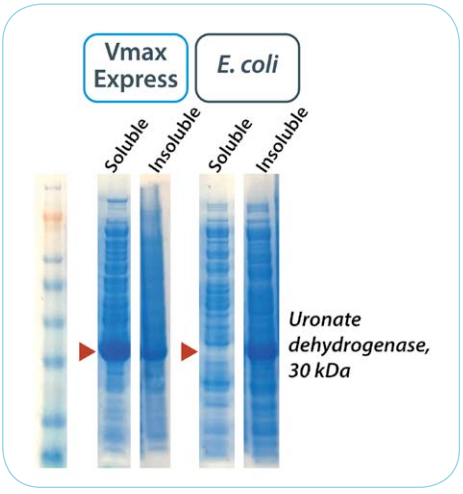

Figure 4. The majority of recombinant protein is visible in the soluble fraction in Vmax Express, in stark contrast to *E. coli*.

Protein	Size (kDa)	BL21 (DE3)	Vmax Express	Comments
Type I PQQ Dehydrogenase	69	✖	✔	Insoluble in BL21. Soluble in Vmax up to 24 hr post-induction.
DHG Dehydrogenase	25	✔	✖	Protein expressed in BL21. Minimal protein detected in Vmax.
Alditol Oxidase	41	✔	✔+	Expressed in both. More protein and biomass using Vmax.
GFP	27	✔	✔+	Expressed in both. More protein and biomass using Vmax.
Glucose Dehydrogenase	40	✔	✔+	Expressed in both. More protein and biomass using Vmax.
Uronate Dehydrogenase	30	✖	✔	Insoluble in BL21. Soluble in Vmax up to 24 hr post-induction.

Table 1. Superior recombinant protein expression in Vmax Express cells.

Conclusions

For largely historical reasons, *E. coli* is the most commonly used bacterial strain for molecular biology. To overcome challenges with *E. coli*, incremental improvements in the strains and expression protocols have been made over the past few decades. Despite these modifications, challenges such as low levels of expression and poor solubility often persist for specific proteins. Vmax Express is a novel bacterial host strain derived from a marine bacterium with a doubling time twice as fast as *E. coli*. With the ability to generate larger amounts of biomass per volume of cells, Vmax Express can produce greater amounts of protein. Compared to *E. coli*, Vmax Express yields substantially higher levels of soluble protein faster for most proteins tested. Because it is compatible with growth media, plasmids, and workflows commonly used for *E. coli*, Vmax Express is a convenient alternative for prokaryotic recombinant protein expression and may help avoid problems frequently encountered with other prokaryotic expression systems.

SGI-DNA Vmax™ Express Electrocompetent Cells

SGIDNA
A Synthetic Genomics, Inc. Company

Rationally Engineered Protein Expression Cells Designed to Accelerate Workflows and Avoid Problems Often Encountered with *E. coli*

- **Improved yields —** produce up to 2X biomass and 4X soluble protein
- **Faster results —** transformation to protein purification in three days
- **Seamlessly switch from *E. coli* —** compatible with media and vectors

US ONLY

Vmax Express is a fast-growing, novel bacterial host optimized for recombinant protein expression. Using a workflow similar to that of *E. coli,* Vmax Express cells are compatible with commonly used expression vectors, antibiotics, and growth media. With a doubling time twice as fast as *E. coli,* Vmax Express can produce more biomass and protein faster.

Description	Size	Cat. No.	Unit
Vmax Express Electrocompetent Cells	5 Rxn	**75997-592**	**Each**
Vmax Express Electrocompetent Cells	10 Rxn	**75997-594**	**Each**
Vmax Express Electrocompetent Cells	20 Rxn	**75997-596**	**Each**
Vmax Enriched Growth Media	1 L	**75997-598**	**Each**

These products are not available in Canada. Please contact your VWR Sales Rep to learn about easy access to similar options in your region.

VWR® COLLECTION designed for your space

Diagram of a **Lab Chair**

Whatever the industry, whatever the application, VWR can help you assess the ergonomic seating needs of your workers to find what best fits your requirements. We offer laboratory seating, task chairs, benches, office seating, and cleanroom chairs, as well as step stools and ladders.

Ergonomic lab seating makes your employees comfortable throughout the workday, and in turn, more productive. Our office seating selection is attractive, ergonomic, and complements office decor. If you must protect your work environment from particulate contamination and/or damage from unwelcome static charges, you'll find the perfect chairs in the cleanroom chairs section.

Chair Features

A. Plastic panel protects upholstery

B. Contoured foam cushioned seat and back

C. Ergonomic controls with all adjustments easily made from the seated position with paddles

D. Positive-grip, adjustable footring will not slip or sag

E. Top-of-the-line pneumatic adjustment mechanism; guaranteed for life

F. Heavy-duty base components meet all ANSI and BIFMA ratings

G. Dual-wheel, polyurethane casters for hard floors

Adjustable armrests support the forearm and wrist (not shown)

VWR Five-Year Chair Warranty

VWR® Contour™ lab and office seating is covered by a five (5) year warranty against defects in material, workmanship, or abnormal wear. Upholstery is covered for one (1) year. Pneumatic cylinders are covered for life. Complete warranty details are available from your VWR Sales Representative.

For help selecting the chair that best fits your needs, visit vwr.com/chair-builder

VisiGlo™ Prime and VisiGlo Select HRP Chemiluminescent Substrates Offer Long Lasting, Highly Sensitive Detection for Western Blotting

Many life science researchers rely on Western blot analysis to evaluate protein levels, integrity, and function. Western blotting is highly versatile and can be used for experiments ranging from initial analyses to validation. The procedure involves the separation of proteins by size on a gel matrix, transfer and immobilization onto a membrane, and incubation with a labelled antibody that binds to the protein of interest.

The most commonly employed reporter label is horseradish peroxidase (HRP), an enzyme whose activity is monitored by the generation of a visible product. The substrate for HRP can be one of many commercially available products, either chromogenic or chemiluminescent, although the chemiluminescent substrate is more widely preferred because of its higher sensitivity. However, not all chemiluminescent substrates perform equally.

Selecting an appropriate substrate requires consideration of several critical factors such as the abundance of the desired protein, stability of the HRP signal, and sensitivity of the HRP substrate system. VWR Life Science AMRESCO offers three levels of chemiluminescent substrates suitable for the detection of HRP labelled proteins in various experimental conditions: VisiGlo Select for ultimate sensitivity with low abundance proteins; VisiGlo Prime for high sensitivity and extended signal duration; and VisiGlo HRP for medium to high abundance proteins.

Each VisiGlo substrate is formulated to achieve maximum signal to noise ratios and is compatible with both x-ray film and CCD-based imaging systems. VisiGlo Select may also be used with fluorescence-based imagers for greater detection flexibility. Although VisiGlo HRP requires cold storage, both VisiGlo Prime and VisiGlo Select are stable when stored at room temperature.

METHODS

Cell Culture

K562 cells were cultured in RPMI 1640 supplemented with 10% fetal calf serum, 100µg/mL streptomycin and 100 IU/mL penicillin. The cells were grown in a 37°C humidified incubator with 5% CO_2 until ready for harvesting.

Protein Isolation

K562 cells were re-suspended in growth media and transferred to a centrifuge tube, then pelleted and washed once in PBS. VWR Life Science AMRESCO's Cytoplasmic/Nuclear Protein Enrichment Kit was used according to the manufacturer's protocol to isolate protein from 5 x 10^6 cells. Aliquots of protein were stored frozen until ready for use.

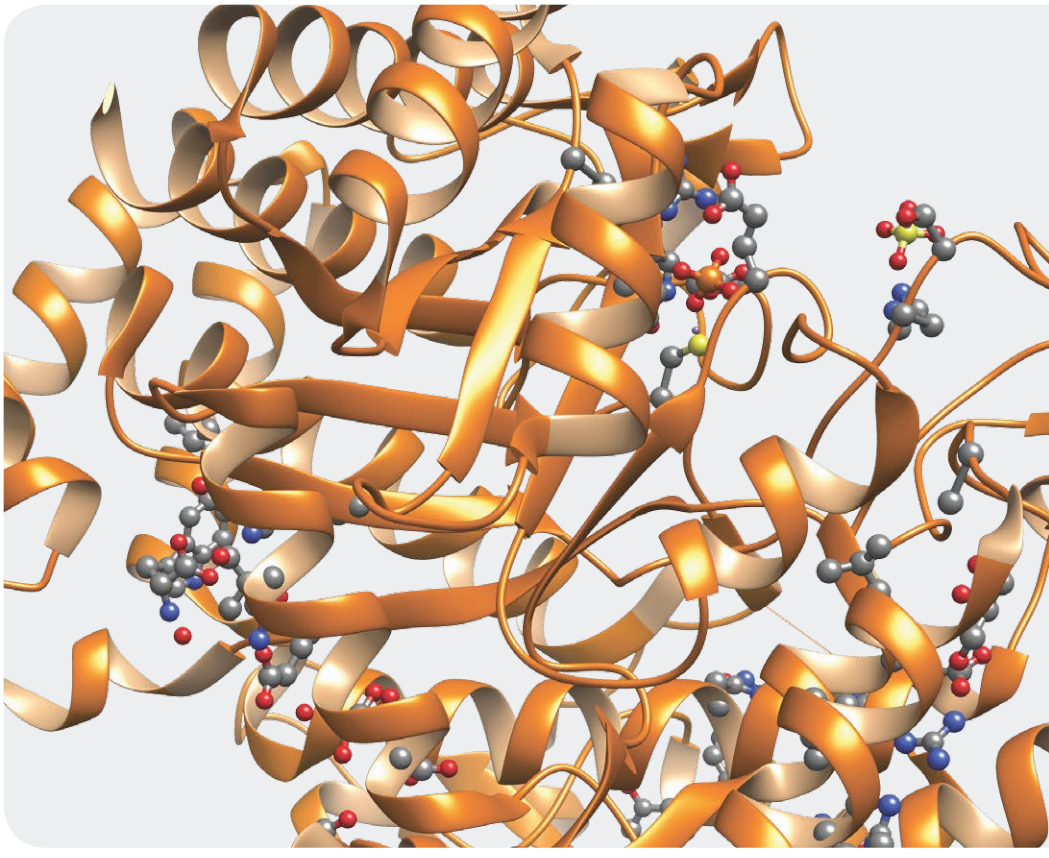

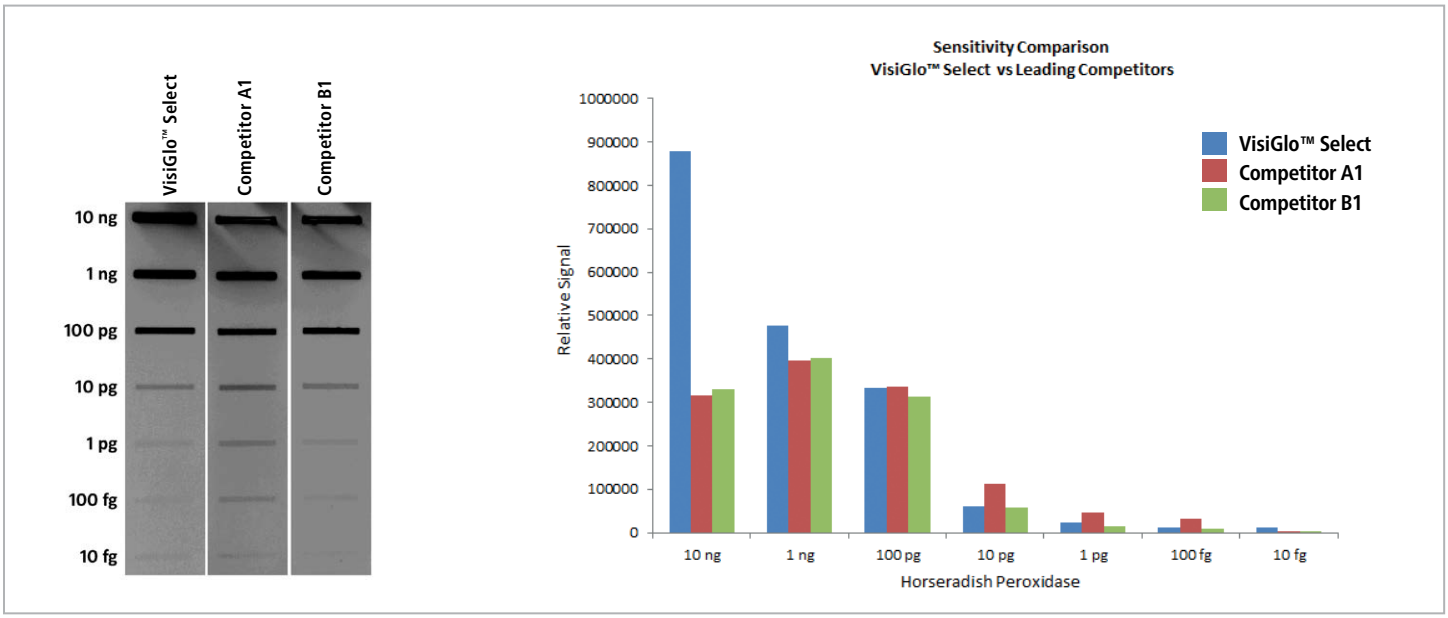

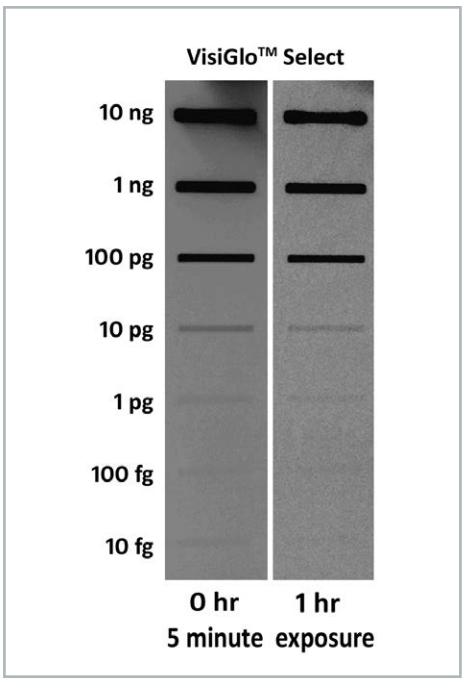

Figure 1. Sensitive HRP detection with VisiGlo Select.
A) Identical slot blots with 10-fold serial dilutions of horseradish peroxidase (10ng–10fg) were incubated separately in three chemiluminescent substrates for comparison: VisiGlo Select HRP Chemiluminescent Substrate Kit, Competitor A1, and Competitor B1. Sensitivity down to 10fg HRP was observed in all lanes.
B) Signal intensities for each HRP concentration were quantitated in ImageQuant (Molecular Dynamics) and were similar at most levels. VisiGlo Select was the only substrate, however, to maintain high intensity at 10ng, while the other substrates were already partially depleted.

Figure 2. Persistent signal after incubation in VisiGlo™ Select.
The slot blot from Figure 1 was used to capture an exposure at 1 hour following the initial substrate incubation. At all HRP concentrations, the signal was maintained at similar intensity to the original exposure.

Protein Electrophoresis

Cytoplasmic proteins were resolved by SDS-PAGE using VWR Life Science AMRESCO's Fluorescent SPRINT NEXT GEL® 12.5% or by standard Laemmli resolving gels (12%) topped with VWR Life Science AMRESCO's Colored Laemmli Stacking Gel Solution.

Slot Blotting

A Bio-Dot SF apparatus was used to bind proteins onto PVDF membrane by filtration with a vacuum pump.

Protein Transfer

Semi-dry transfer of protein to PVDF was performed using VWR Life Science AMRESCO's Rapid Transfer Buffer, 10X, according to the product instructions, with constant voltage set at 25V and a transfer time of 10 minutes.

Western Blotting and Slot Blotting

Western blots were blocked in TBST/5% non fat dry milk for 1 hour, followed by incubation in primary antibody diluted in blocking solution for 1 hour to overnight. The blot was washed and incubated with an HRP conjugated secondary antibody for an hour. After a final wash, the blot was visualised using VisiGlo or competitors' chemiluminescent substrate kit according to the product instructions. Images were captured using a Syngene G:Box HR gel documentation system.

Slot blots containing serial dilutions of HRP were immediately immersed in chemiluminescent substrate for HRP detection. Slot blots containing serial dilutions of other proteins were processed in the same manner as Western blots.

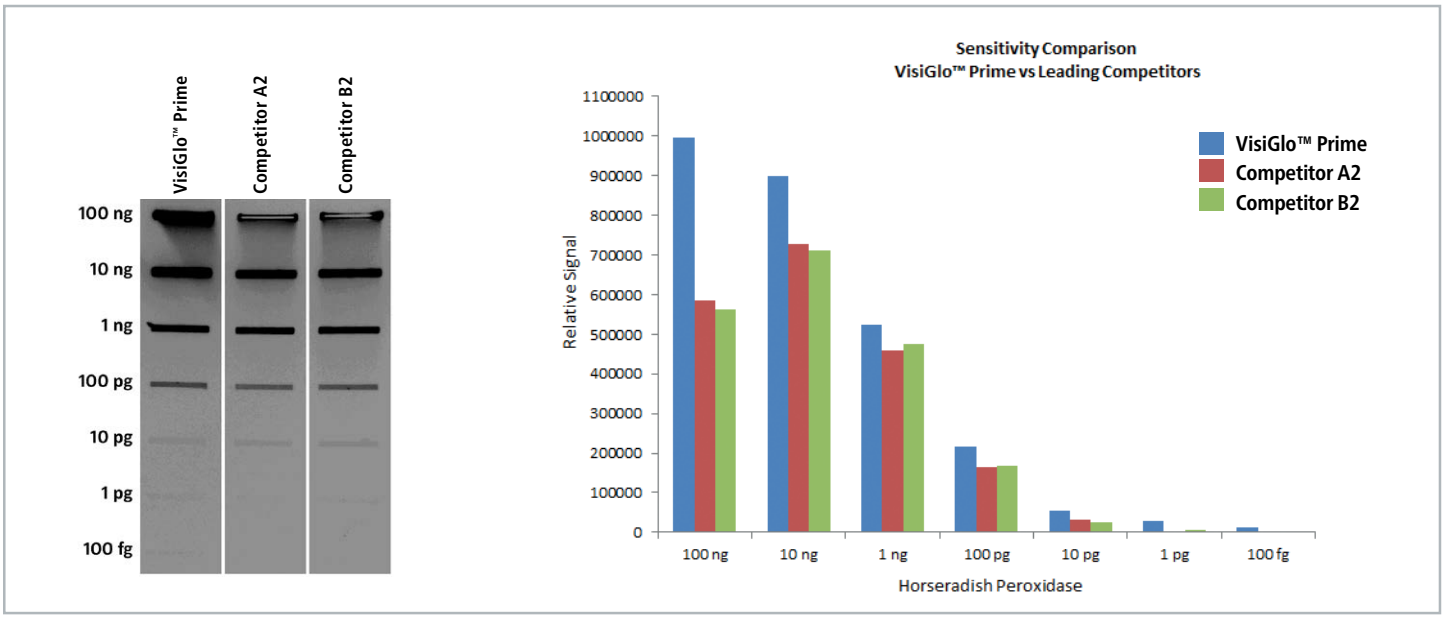

Figure 3. Sensitive and broad linear detection of HRP with VisiGlo Prime.
A) Identical slot-blots with 10-fold serial dilutions of horseradish peroxidase (100ng–100fg) were incubated separately in three chemiluminescent substrates for comparison: VisiGlo Prime HRP Chemiluminescent Substrate Kit, Competitor A2, and Competitor B2. VisiGlo Prime was the only substrate not to exhibit inverse staining of the 100ng HRP band, a phenomenon associated with substrate burn-out. VisiGlo Prime also had greater sensitivity, with a lower limit of HRP detection at 100fg. **B)** Signal intensities for each HRP concentration were quantitated in ImageQuant (Molecular Dynamics) and were similar for all substrates between 10ng and 10pg, but highest for VisiGlo Prime at the highest and lower concentrations.

Quantitation of Signal

Protein band quantitation was performed using ImageQuant 5.2 software.

RESULTS AND DISCUSSION

VisiGlo Select is a premium substrate that combines a broad, linear dynamic range and low femtogram sensitivity to enable quantitation of low abundance, peroxidase labelled proteins. For comparison to other top tier leading substrates, a slot blot with identical lanes of 10-fold HRP dilutions was prepared and divided into strips for development with the different products according to their respective instructions. The blots were imaged with a CCD-based gel documentation system with identical settings and 5 minute exposures. VisiGlo Select, Competitor A1, and Competitor B1 were all capable of detecting as little as 10fg of HRP with these conditions (Figure 1A). Background corrected signal intensities indicate most HRP concentrations produced similar intensity bands with all three substrates (Figure 1B); however, at the highest concentration of 10ng HRP, VisiGlo Select had a much stronger signal (Figure 1A) because the other substrates were showing signs of substrate depletion, observed as very narrow regions of 'ghost banding' in the band centres of the magnified high resolution image (data not shown).

These data indicate that VisiGlo Select can function as a direct replacement for the leading substrates when maximum sensitivity is required and that it is the best choice for detecting labelled proteins present in a broad concentration range from nanogram down to femtogram

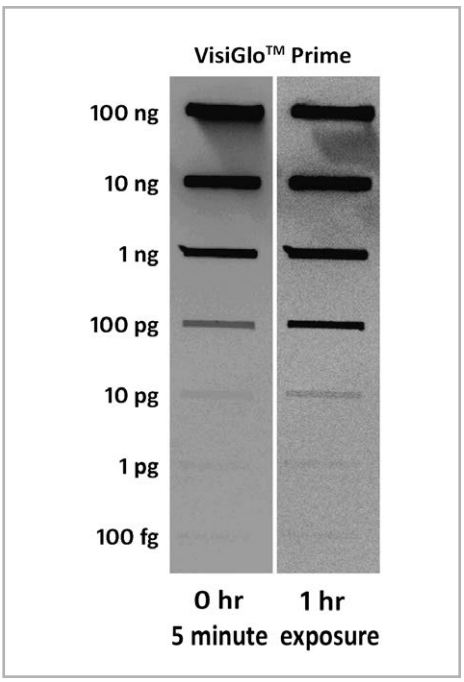

Figure 4. Persistent signal after incubation in VisiGlo Prime.
A slot blot detected with VisiGlo Prime maintained similar signal intensity for all HRP concentrations from initial exposure to 1 hour later.

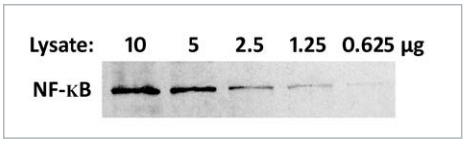

Figure 5. High sensitivity and low background on a Western blot detected with VisiGlo Prime. Serial dilutions of K562 cytoplasmic lysate were resolved by SDS-PAGE and transferred to PVDF using VWR Life Science AMRESCO's Rapid Transfer Buffer. The Western blot was probed with anti-NF-KB (1:2,000) primary and HRP labelled secondary antibodies. VisiGlo Prime HRP Chemiluminescent Substrate was used to detect the target, with NF-KB detected in as little as 625ng of lysate.

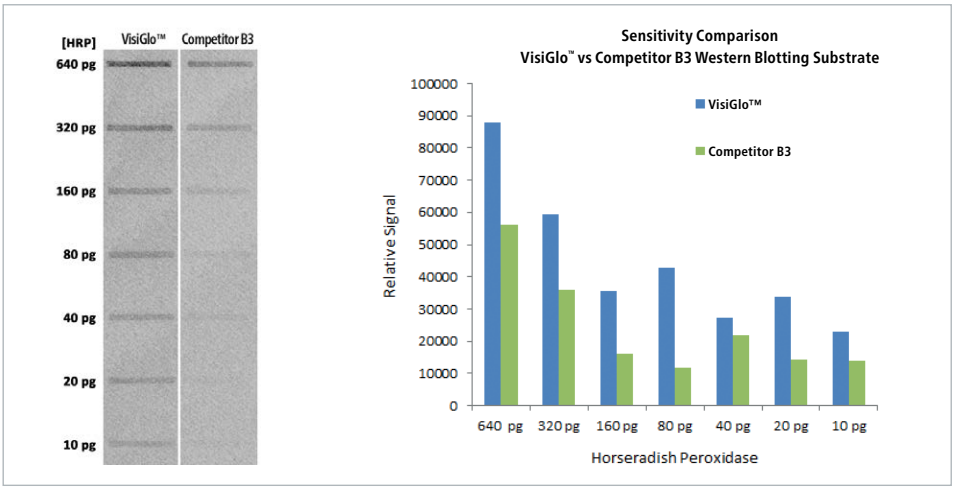

Figure 6. Detection of picogram range HRP with high signal to noise using VisiGlo HRP. **A)** Identical slot-blots with 2-fold serial dilutions of horseradish peroxidase (640pg – 10pg) were incubated separately in two chemiluminescent substrates for comparison; VisiGlo HRP Chemiluminescent Substrate Kit and Competitor B3. Both substrates detected each HRP concentration, however, VisiGlo resulted in higher intensity bands. **B)** Signal intensities for each HRP concentration were quantitated in ImageQuant (Molecular Dynamics) to demonstrate the difference in the product performances.

levels. Additional benefits of VisiGlo Select include its long signal duration of up to 8 hours, which allows for image optimization, as well as its compatibility with film and CCD-based or fluorescence-based gel imaging systems. VisiGlo Select is also stable at room temperature for 1 year.

VisiGlo Prime is a room temperature stable substrate that is ideal for accurate protein quantitation, with a linear dynamic range of signal versus protein concentration ranging over three orders of magnitude. In a direct slot blot comparison with Competitor A2 and Competitor B2, only VisiGlo Prime detected HRP at a level of 100fg and showed no evidence of substrate depletion at 100ng of HRP (Figure 3A, 3B). The chemiluminescent emission from VisiGlo Prime is highly stable, lasting up to 10 hours after substrate incubation, depending on level of HRP present. A 5 minute exposure of the VisiGlo Prime blot 1 hour after initial substrate incubation resulted in a persistent full range of detection without decreased signal or substrate depletion and no significant increase in background (Figure 4). VisiGlo Prime was also used to detect NF-κ in 10µg down to 0.625µg of K562 cytoplasmic lysate by Western blotting, with clear and distinct detection with a 5 minute exposure, even at the lowest concentration (Figure 5).

The original VisiGlo HRP Chemiluminescent Substrate Kit is an excellent and inexpensive option for routine detection of peroxidase labelled proteins present in medium to high abundance. It has sensitivity down to the low picogram range and has been shown to yield a more intense signal than Competitor B3 in identical conditions by slot blotting with HRP (Figure 6A, 6B). VisiGlo HRP produces optimal signal to noise for clear results using CCD- or film-based imaging.

CONCLUSIONS

VisiGlo Select, VisiGlo Prime, and VisiGlo chemiluminescent substrates were matched to equivalent tier substrates from leading competitors and analysed by slot blot to compare sensitivity and signal duration. Although priced lower than the competition, each VisiGlo substrate exhibited comparable or superior performance for sensitivity of detection and background noise. The substrates offer a broad range of detection coverage and are formulated to yield maximum signal to noise ratios in their respective tiers, enabling long exposures without compromising image quality.

US ONLY

Description	Cat. No.	Unit
Visiglo HRP Chemiluminescent ECL Substrate Kit*	97064-146	Each
Visiglo Plus HRP Chemiluminescent ECL Substrate Kit*	97063-148	Each
VisiGlo Select HRP Chemiluminescent ECL Substrate Kit	89424-018	Each
VisiGlo Prime HRP Chemiluminescent ECL Substrate Kit	89424-016	Each

** These products are not available in Canada. Please contact your VWR Sales Rep to learn about easy access to similar options in your region.*

Air Samplers for Microbial Control and Monitoring of Air Quality

HARDY DIAGNOSTICS
A Culture of Service™

Introducing TRIO.BAS™: The Next Generation in Viable Airborne Particle Sampling

- Portable air sampling for enviromental/cleanroom monitoring
- Uses standard 100mm or 60mm media plates
- Instruments can transfer data via Bluetooth® technology
- Balanced and lightweight design
- 100L/min and 200L/min air flow rate models available

Controlled air flow from the TRIO.BAS sampling instrument, passing through an aspirating head, impacts onto an appropriate agar plate that collects bacteria and other organic substances possibly present in the sampling area. Contact your VWR Sales Rep for more information on the Mini, Duo, Trio, Isolator, or Gas models.

Description	Capacity	Cat. No.	Unit
TRIO.BAS Mono Contact Plate	100L/min	**75804-708**	**Each**
TRIO.BAS Mono Petri Plate	100L/min	**75804-710**	**Each**
TRIO.BAS Mono Contact Plate	200L/min	**75804-712**	**Each**
TRIO.BAS Mono Petri Plate	200L/min	**75804-714**	**Each**
Base Station Induction Battery Charger		**75928-106**	**Each**
Accessories			
Stainless Steel Aspirating Head, Contact Plate		**75804-746**	**Each**
Sterile Polystyrene Daily Shift Head, Contact Plate		**75804-756**	**Each**
Stainless Steel Aspirating Head, Petri Plate		**75804-748**	**Each**
Sterile Polystyrene Daily Shift Head, Petri Plate		**75804-758**	**Each**

BioGems Small Molecules

biogems
A PeproTech Brand

PEPROTECH
OUR SUPPORT, YOUR DISCOVERY

Premium Quality Life Science Research Reagents

- Guaranteed high purity and lot-to-lot consistency
- Precisely manipulate key biological pathways
- Biological effects are typically rapid, reversible, and dose-dependent

US ONLY

Small Molecules are low molecule weight organic compounds that allow for the finer control of cellular responses. Their small size allows them to diffuse rapidly across cell membranes to reach intracellular sites of action. BioGems targeted catalog also includes the most important reagents for stem cell research that can be used to direct cellular differentiation, reprogramming, or self-renewal.

Description	CAS No.	Size	Cat. No.	Unit
Brefeldin A	20350-15-6	25 mg	**75844-590**	**Each**
Chir 99021	252917-06-9	10 mg	**75844-610**	**Each**
Forskolin	66575-29-9	50 mg	**75844-686**	**Each**
PD 0325901	391210-10-9	25 mg	**75844-618**	**Each**
Puromycin Dihydrochloride	58-58-2	500 mg	**75844-854**	**Each**
SB 431542	301836-41	10 mg	**75844-602**	**Each**
Valproic Acid, Sodium Salt	1069-66-5	100g	**75844-938**	**Each**
Y-27632 Dihydrochloride	129830-38-2	10 mg	**75844-614**	**Each**

These products are not available in Canada. Please contact your VWR Sales Rep to learn about easy access to similar options in your region.

SMART Digest Compared to Classic In-Solution Digestion of Rituximab for In-Depth Peptide Mapping Characterization

By Martin Samonig[1], Alexander Schwahn[2], Ken Cook[3], Mike Oliver[4], and Remco Swart[1]

[1]Thermo Fisher Scientific, Germering, Germany; [2]Thermo Fisher Scientific, Basel, Switzerland; [3]Thermo Fisher Scientific, Hemel Hempstead, United Kingdom; [4]Thermo Fisher Scientific, Runcorn, United Kingdom

INTRODUCTION

Peptide mapping is a common technique in the biopharmaceutical industry to characterize monoclonal antibodies (mAbs) for the determination of product identity and stability. Many conventional sample preparation methods are time consuming with digestion times of several hours and can introduce modifications such as deamidation, oxidation, and carbamylation[1]. In this study, two classic in-solution digestion approaches were compared to the recently developed SMART Digest kit method to quantify the extent of post-translational and chemical modifications of a therapeutic recombinant mAb. The critical requirements for each method were the complete sequence coverage of the heavy and light chain and the accurate identification and (relative) quantification of the glycans attached to the asparagine 301 on the heavy chain. Deamidation, oxidation, and carbamylation are induced primarily during sample preparation and were thus monitored for a direct comparison of the different digestion methods. A time course experiment for the SMART Digest was performed to assess the influence of digestion time on modification formation.

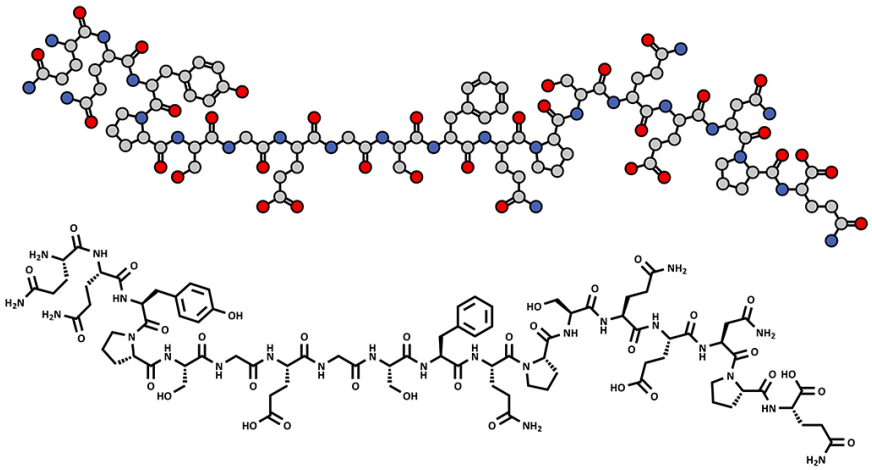

EXPERIMENTAL

Consumables

- Thermo Scientific Acclaim VANQUISH C18, 2.2µm, 2.1 × 250mm (Cat. No. 10043-322)
- Thermo Scientific SMART Digest Kit (Cat. No. 60109-101)
- LCMS Grade Water
- LCMS Grade Acetonitrile
- LCMS Grade Trifluoroacetic Acid
- LCMS Grade Formic Acid
- MS Grade Trypsin Protease
- DTT (Dithiothreitol)
- Urea
- Iodoacetamide
- Ultrapure Grade Tris Hydrochloride

Sample Pretreatment and Sample Preparation

A commercially available monoclonal antibody rituximab drug product (Hoffmann La Roche, Basel, Switzerland) was supplied at a concentration of 10mg/mL in a formulation buffer containing 0.7mg/mL polysorbate 80, 7.35mg/mL sodium citrate dehydrate, 9mg/mL sodium chloride, and sterile water adjusted to pH 6.5 using sodium hydroxide.

In-Solution Digestion Protocol Using Urea for Denaturation

Rituximab (400µg) was denatured for 75 min in 7M urea and 50mM tris hydrochloride (HCl) at pH 8.0, followed by a reduction step using 5mM dithiothreitol (DTT) for 30 min at 37°C. Alkylation was performed with 15mM iodoacetamide (IAA) for 30 min at room temperature and the reaction was quenched by addition of 9mM DTT. The sample was then diluted 1:10 (v/v) with 50mM tris HCl pH 8.0 to reach a final urea concentration below 1M. Trypsin was added with a protein/protease ratio of 40:1 (w/w) and digestion was allowed to proceed overnight at 37°C. Digestion was stopped by the addition of trifluoroacetic acid (TFA) to a final concentration of 0.5%. (Sample name: In-Solution, Urea)

In-Solution Digestion Protocol Using Heat for Denaturation

Rituximab (400µg) was denatured in 50mM tris HCl at pH 8.0 and 70°C for 75 min, followed by a reduction step using 5mM DTT for 30 min at 70°C. Alkylation was performed with 15mM IAA for 30 min at room temperature and the

thermo scientific

reaction was quenched by addition of 9mM DTT. The sample was then diluted 1:10 (v/v) with 50mM tris HCl pH 8.0. Trypsin was added with a protein/protease ratio of 40:1 (w/w) and digestion was allowed to proceed overnight at 37°C. Digestion was stopped by addition of TFA to a final concentration of 0.5%. (Sample name: In-Solution, Heat)

SMART Digest Kit Protocol

The 50µL rituximab sample, adjusted to 2mg/mL with water, was diluted 1:4 (v/v) with the SMART Digest buffer provided with the kit. It was then transferred to a reaction tube containing 15µL of the SMART digest resin slurry, corresponding to 14µg of heat-stabile, immobilized trypsin. A time course experiment was performed and tryptic digestion was allowed to proceed at 70°C for 15, 30, 45, and 75 min at 1400 rpm; a digestion time of 45–60 min was found to be sufficient to achieve digestion completeness for mAb samples. After the digestion, the reaction tube was centrifuged at 7000 rpm for 2 min, the supernatant was transferred to a new tube, and the centrifugation step was repeated. Disulfide bonds were reduced by incubation for 30 minutes at 37°C with 5mM DTT. (Sample names: SMART Digest, 15, 30, 45, 75 min)

All samples were diluted with 0.1% formic acid (FA) in water to a final protein concentration of 100ng/µL and 2.5µg were loaded on the column for all runs.

LC CONDITIONS

Instrumentation

Vanquish Flex Quaternary System
Separation conditions (unless noted otherwise in the text)

Column: Acclaim VANQUISH C18, 2.2µm, 2.1 × 250mm
Mobile Phase A: Water + 0.1% FA
Mobile Phase B: Water/acetonitrile (20:80 v/v) + 0.1% FA
Flow Rate: 0.3 mL/min
Temperature: 50°C, Forced air mode
Gradient: See Figure 1

MS CONDITIONS

Instrumentation

The Thermo Scientific Q Exactive HF mass spectrometer (MS) was used for detection.

Data Processing

The data were acquired with the Thermo Scientific™ Chromeleon™ Chromatography Data System, version 7.2 SR4. Thermo Scientific™ BioPharma Finder™ software, version 1.0 SP1, was used for data analysis.

RESULTS AND DISCUSSION

The SMART Digest kit provides fast and simple protein digestion with outstanding reproducibility, and digestion completeness for mAb samples is typically achieved within 45–60 min (Figure 2). Here, the relative standard deviation (RSD) was used to evaluate reproducibility, as demonstrated in Figure 3 (next page). Three separate digestions of the same mAb sample were conducted by three different analysts on different days. The peptide maps generated perfectly overlap with an average RSD for the peak area of less than 5%. These results

Time [min]	A[%]	B[%]	Flow Rate [mL/min]
0.0	96	4	0.3
50.0	25	75	0.3
51.0	0	100	0.3
60.0	0	100	0.3
61.0	96	4	0.3
80.0	96	4	0.3

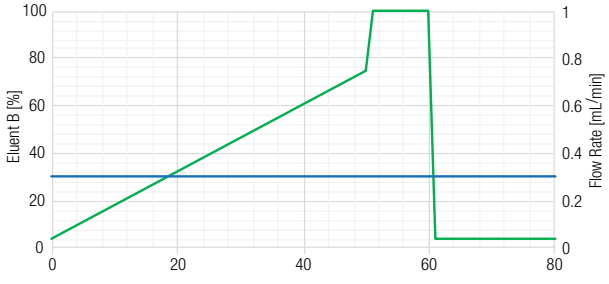

Figure 1. LC gradient.

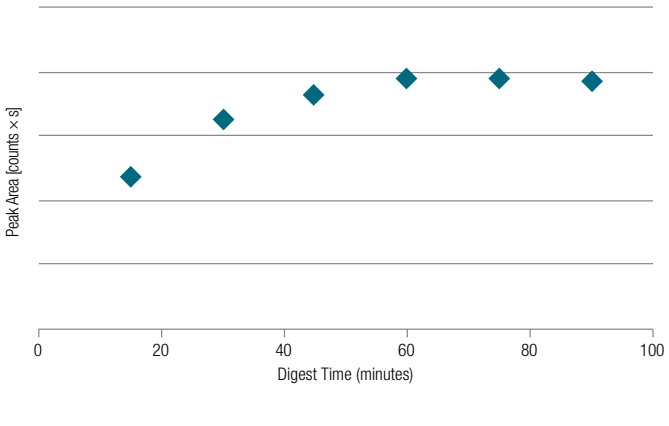

Figure 2. IgG digest profile, monitoring the mAb peptide VVSVLTVLHQDWLNGK for digestion times from 15–90 min using the SMART Digest kit.[2]

impressively highlight the reproducibility that can be achieved when using this novel digestion technique in combination with the Vanquish Flex UHPLC system featuring SmartInject, the intelligent sample pre-compression technology for class-leading retention time reproducibility.

Comparing the total ion current (TIC) chromatograms of an in-solution-digested sample and a SMART Digest sample (Figure 4) shows the similarity of the two digestion methods. The 75 min time point was chosen to mirror the elongated incubation time of an overnight digest.

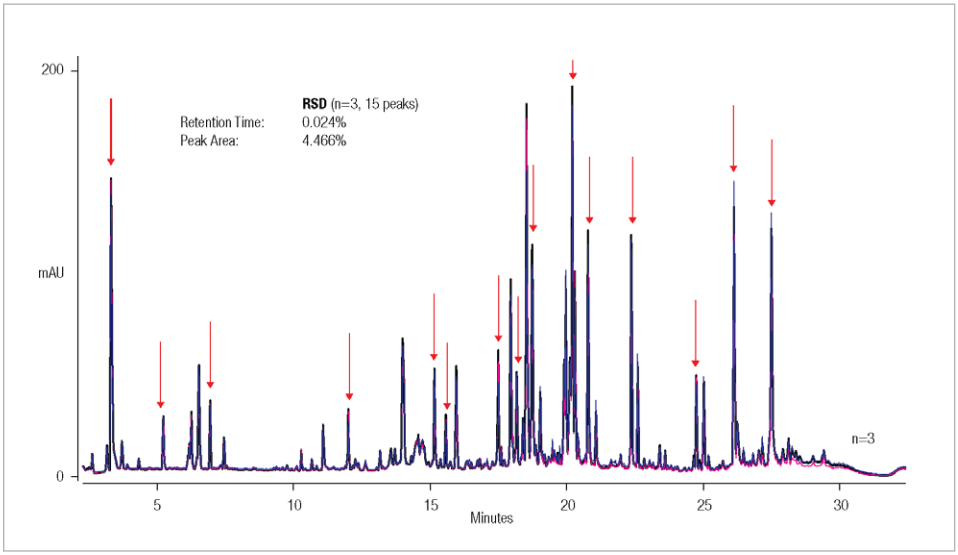

Figure 3. UV chromatogram overlay from three separate SMART digestions from the same mAb, conducted by three individual operators. The 15 marked peptides in each sample were used for inter-user/inter-day RSD value calculations.

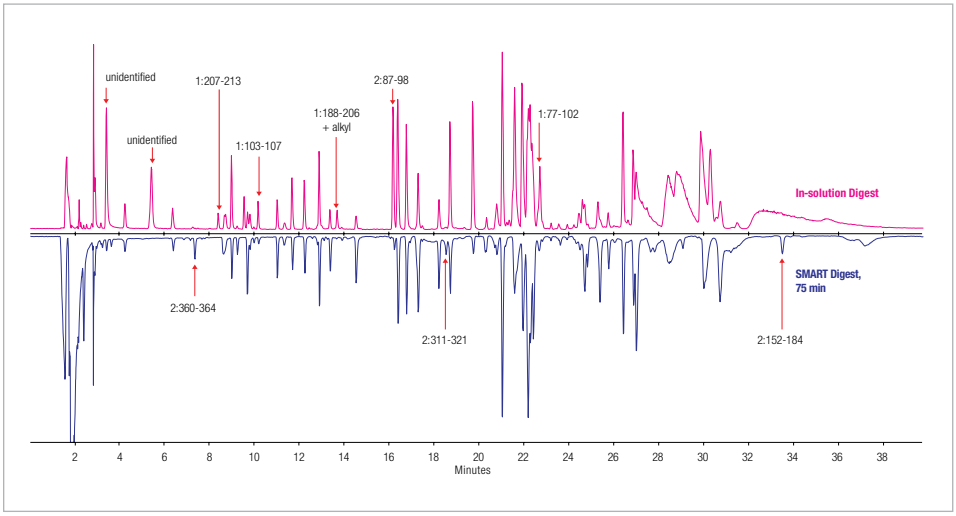

Figure 4. Mirror plot of the TIC chromatogram for the in-solution-digested sample denatured with heat *(In-Solution, Heat)* and the reduced SMART Digest sample *(SMART Digest, 75 min).* Peak labels give annotation to light (1) or heavy (2) chains, respectively, and sequence position.

In general, the peptide pattern is homogenous and most of the detected peptides are aligned.

Differences in the two chromatograms and identified peptides are highlighted. For some peptides, the intensity slightly differs between the two SMART and in-solution digest runs, for example, peptides "1:103–107" and "2:87–98". Others appear in only one of the two digestion methods, such as alkylated peptides "1:188–206 + alkyl". The injection peak eluting with the void volume of the SMART Digest sample is higher in comparison to the in-solution-digested sample and is caused by salt components included in the SMART Digest buffer to optimize the digestion efficiency at elevated temperatures. This peak did not affect the result of the peptide map but could be easily removed if required. One option is to use a post-column diverter valve prior to the MS ion source. Another is to use Thermo Scientific™ SOLAμ™ SPE plates that allow highly reproducible post-digestion desalting of peptide samples by solid phase extraction (SPE)[3].

In peptide mapping analysis of mAbs, 100% sequence coverage for the heavy and light chains must be achieved. The sequence coverages for the different digest conditions are shown in Table 1. For all six methods, including the fast digestion methods of 15 and 30 min, 100% coverage was achieved for light as well as heavy chains. Strikingly, an incubation time of only 15 min is sufficient to achieve 100% sequence coverage for both the heavy and light chains of the antibody when the SMART Digest kit is used. The number of detected MS peaks in the samples digested with the SMART Digest kit were generally higher than in the in-solution digested samples. The same trend was observed when the number of identified components, including all peptides and charge states, and the total MS ion count were compared (Table 2).

thermoscientific

Peptide mapping experiments can provide the identification, localization, and (relative) quantification of various post translational and chemical modifications (PTMs) that might be present on the amino acid residues. The relative abundance of all identified modifications (n=85) in the different runs are plotted in Figure 5. The relative abundance of the major modifications, including the pyro-glutamate formation (NH_3 loss) on the N-terminal glutamine of heavy as well as light chain and the most abundant glycoforms attached to the asparagine 301 of the heavy chain (A2G1F, A2G0F, and A2G2F), are shown in Figure 5. Sixteen cysteine carbamidomethylation sites were exclusively identified in the samples derived from the in-solution-digested samples but not in the SMART Digest. This is consistent with the modification being caused by the alkylation with IAA during the sample preparation. For simplicity, the carbamidomethylation sites are not shown in Figure 5. Overall, similar levels for all modifications were detected for all digest protocols and no significant trend of an increased or decreased amount in any of the conditions tested was observed. Noteworthy, for many modification sites, e.g., deamidation of N319 and oxidation of W106, the amount in the reduced SMART Digest samples were lower compared to the in-solution-digested samples even when a 75 min (over-)digestion with the SMART Digest was applied.

The monoclonal antibody rituximab used in this study consists of 1328 amino acid residues including 16 disulfide bonds[4]. Amongst several potential PTMs of amino acids, deamidation of asparagine or glutamine and oxidation of methionine or tryptophan represent common chemical modifications for mAbs during downstream processing and storage. Figures 6A and 6B show the extent of amino acid oxidation, and deamidation,

Proteins	Number of MS Peaks	MS Peak Area	Sequence Coverage	Relative Abundance	Sample
1: Rituximab Light Chain	521	26%	100%	40%	*SMART Digest, 15 min*
	532	24%	100%	38%	*SMART Digest, 30 min*
	526	22%	100%	38%	*SMART Digest, 45 min*
	516	19%	100%	36%	*SMART Digest, 75 min*
	404	28%	100%	37%	*In-Solution, Urea*
	407	31%	100%	38%	*In-Solution, Heat*
2: Rituximab Heavy Chain	827	43%	100%	54%	*SMART Digest, 15 min*
	833	47%	100%	56%	*SMART Digest, 30 min*
	827	45%	100%	55%	*SMART Digest, 45 min*
	855	37%	100%	59%	*SMART Digest, 75 min*
	638	54%	100%	62%	*In-Solution, Urea*
	619	52%	100%	61%	*In-Solution, Heat*

Table 1. Sequence coverage with different digestion methods.

# Identified Components	Total MS area [counts × s]	Sample
1702	3.48×10^9	*SMART Digest, 15 min*
1678	4.12×10^9	*SMART Digest, 30 min*
1688	3.96×10^9	*SMART Digest, 45 min*
1551	3.13×10^9	*SMART Digest, 75 min*
1171	3.65×10^9	*In-Solution, Urea*
1145	4.04×10^9	*In-Solution, Heat*

Table 2. Number of identified components and TIC area for the different runs.

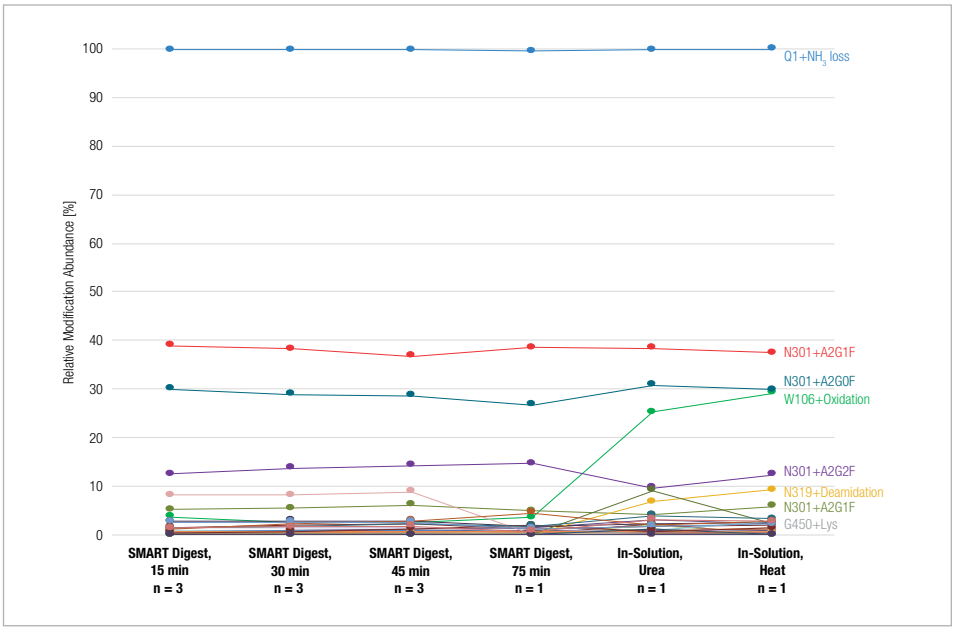

Figure 5. Relative abundance of 85 identified modifications including oxidation, double oxidation, glycation, glycosylation, NH_3 loss, isomerization, lysine truncation, methylation, dimethylation, and carbamylation.

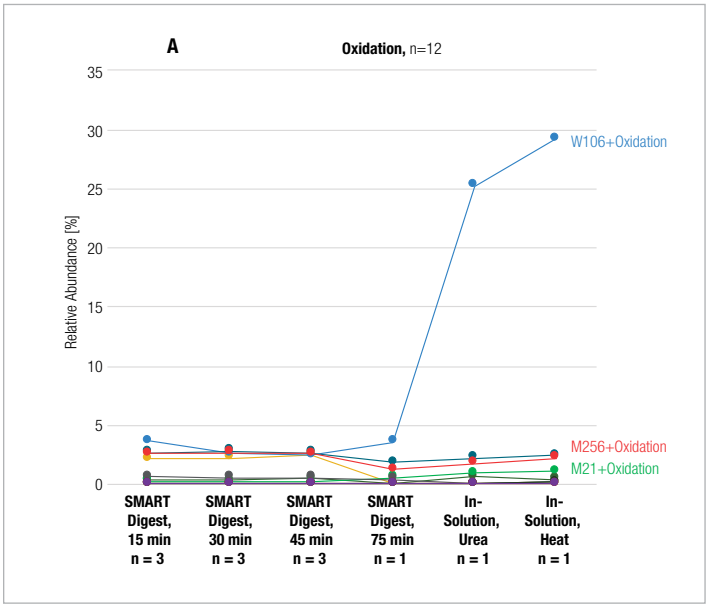

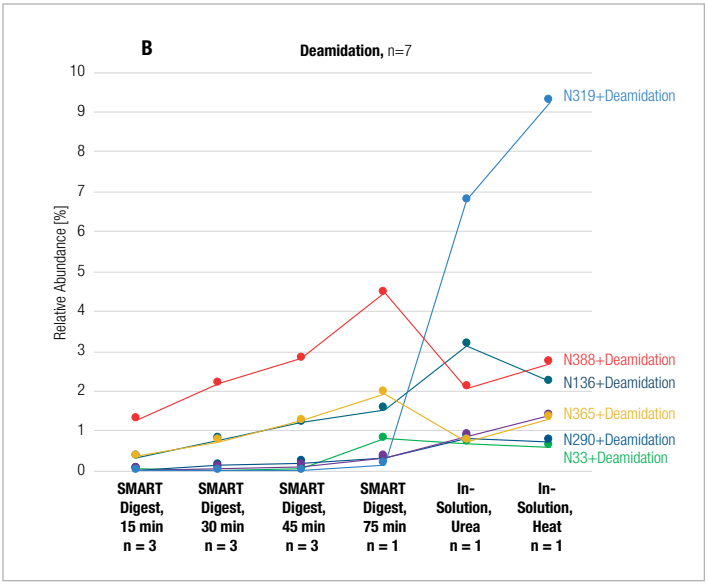

Figure 6. Relative abundance of 12 identified oxidations **(A)** and 7 deamidations **(B)** in different runs with various digestion methods.

respectively, for oxidations for the different digestion methods. Table 3 (page 18) summarizes the quantification results for the individual modification sites. The variance between the six digestion methods is expressed as the RSD of the measured relative abundance for each modification with each of the digestion protocols. With the exception of the oxidation of W106 that was high in the in-solution-digested samples, all results are comparable, resulting in RSD values ≤1%. For the identified deamidations, the maximum RSD value was 3.164% and with an average RSD of 0.913%. While a clear trend of increased deamidations with increasing sample incubation time could be observed between the six digestion methods (Figure 6B), less or equal amounts of deamidation were observed when the SMART Digest kit was used at the recommended digestion time of ≤45 min (Figure 6B and Figure 7). Only two deamidation sites (N236 and N388) were more prone to undergo deamidation under the SMART Digest conditions and required a reduced incubation time of 30 min. Another critical modification is the carbamylation of lysine residues and protein N-termini (+43.006 Da), which is a non-enzymatic PTM that has been related to protein aging[5].It can be artificially introduced during sample preparation using urea as the protein denaturing agent. For in-solution tryptic digest with urea in the sample preparation, the average carbamylation of lysine was ≤1% relative abundance (n=6). For the SMART Digest samples, the average carbamylation was considerably lower in the ppt range or not detectable at all (Table 3). Other commonly targeted modifications such as the presence/absence of a C-terminal Lys, the N-glycosylation of asparagine on the heavy chain, the N-terminal pyro-glutamine formation on heavy and light chains, and lysine glycations are listed in Table 3. In total, six lysine glycations and 12 glycosylations of N301 could be identified and (relatively) quantified with an average RSD value of 0.423%.

Based on all identified oxidations (n=12) and deamidations (n=7), the deamidation and oxidation factor was calculated for each individual sample (Figure 7). The in-solution-digested sample with heat denaturation had the highest induced modification rate of the compared methods, with a deamidation factor of 8.754 and an oxidation factor of 2.923. In contrast, the SMART Digest samples that were reduced on peptide level showed the lowest levels of deamidation and oxidation compared to both in-solution-digestion samples. The degree of deamidation increases with extended digestion times, and the lowest deamidation rate was observed for the sample digested for 15 min using the SMART Digest kit. Deamidation is, in general, accelerated at high temperatures and high pH values[6].One way to minimize the degree of induced deamidation is to lower the pH of the digestion buffer. SMART Digest is performed at elevated temperatures but at a pH of 7.2, which is much lower than the pH of classical in-solution-digestion methods. Thus, deamidation is minimized and is comparable to that observed for standard in-solution digests at 37°C. Figure 5 also demonstrates that the extent of deamidation is location dependent. For some positions, lower levels of deamidation are observed for the SMART Digest, even

thermoscientific

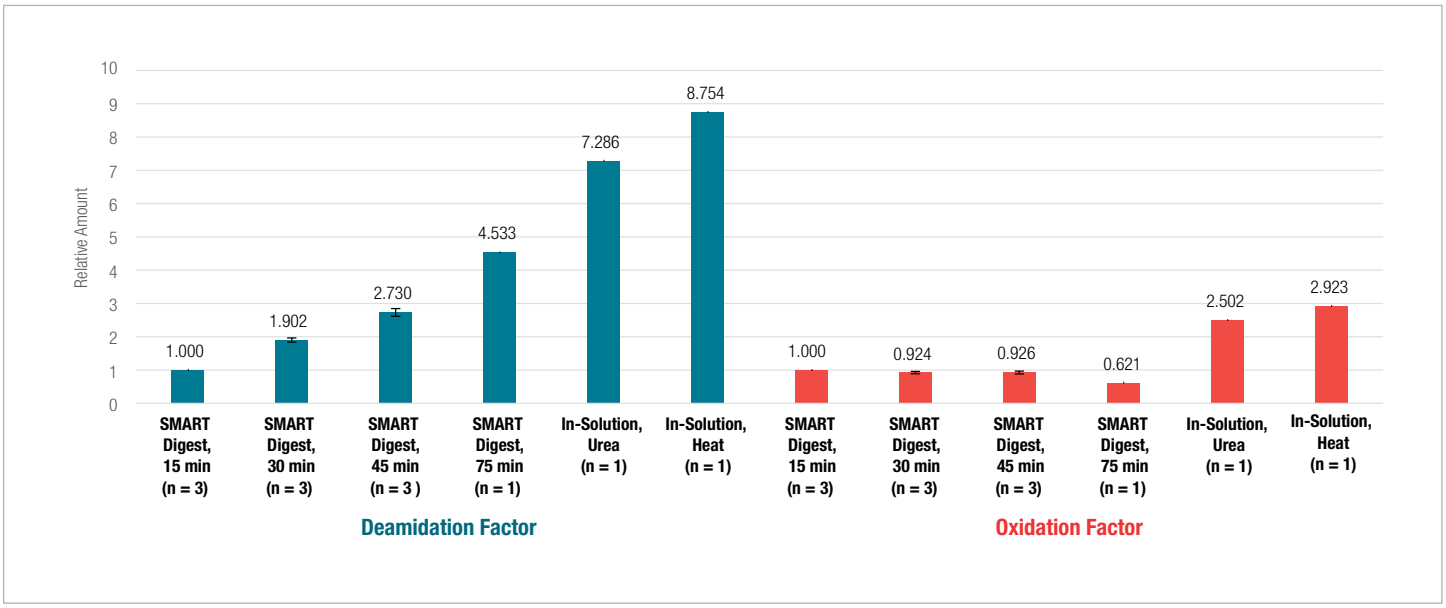

Figure 7. Relative amount of total deamidation and oxidation modifications measured for the six different digest conditions *(Normalization to SMART Digest, 15 min).*

when compared to the urea-treated in-solution digest (e.g., N33, N136, N319). For others, higher levels are observed with the SMART Digest and digestion times ≥45 min (e.g., N388).

Two of the tryptic peptides from rituximab have been identified as the most susceptible to deamidation under stress conditions[7]. The peptides 2:V306-K 321 (VVSVLTVLHQDWLNGK), containing N319, and 2:G375-K396 (GFYPSDIAVEWESNGQPENNYK), containing N388, are both located within the Fc region of the heavy chain, which shares the same sequence with other human or humanized mAbs. More than one asparagine is present in the sequences, but the asparagines highlighted in bold are identified as deamidation hot spots.[7] The second peptide is known as the "PENNY peptide", but both peptides are a decent indicator for induced deamidation of mAbs.[7]

Figure 8 (page 19) shows the TIC chromatogram for the SMART Digest sample (Figure 8A) and extracted ion current (XIC) chromatograms with a 5ppm mass extraction window for the different samples (Figure 8B). The XIC traces in blue are derived from the native 2:V306-K321 peptide present in all runs. The traces in red are the corresponding deamidated forms of the peptide (N319) eluting prior to the native peptide in the chromatogram. The relative abundance, based on all charge states of the deamidated peptide, is lowest in the 15 min digested SMART Digest sample at 0.001%. In contrast, a higher amount of deamidation (N388) was observed with the SMART Digest (45 and 75 min digestion time) for the PENNY peptide 2:G375-K396 (Table 3), but the lowest value of 1.267% could be observed with the 15 min method.

As shown in Figure 8C, the isotopic distribution of the triply charged native peptide is different from its deamidated form. The monoisotopic peak is highlighted in bold and, due to coelution of the two species, the monoisotopic peak (*; m/z 603.340) of the native peptide is also visible in the lower mass spectrum. A deamidation leads to a theoretical mass increase for the monoisotopic peak of 0.984Da, which results in a mass shift of 0.328Da for the triply charged signal and nicely correlates with the measured value.

CONCLUSION

The direct comparison of the SMART Digest kit with the conventional in-solution protein digestion methods conducted in this study showed no substantial difference for the mAb rituximab between the different approaches with respect to the data quality and information content obtained. Protein sequence coverage of 100% for rituximab was achieved with all six digestion methods tested and could be achieved in only 15 min when using the SMART Digest kit. The most common PTMs targeted for analysis, such as the presence/absence of a C-terminal Lys, the N-glycosylation of asparagine on the heavy chain, and the N-terminal pyro-glutamine formation on heavy and light chains, were identified, relatively quantified, and compared between the different digestion

Relative Abundance [%]											
SMART Digest, 15 min (n=3)	SMART Digest, 15 min, RSD (n=3)	SMART Digest, 30 min (n=3)	SMART Digest, 30 min, RSD (n=3)	SMART Digest, 45 min (n=3)	SMART Digest, 45 min, RSD (n=3)	SMART Digest, 75 min (n=1)	In-Solution, Urea (n=1)	In-Solution, Heat (n=1)	RSD (%)*	Median (%)*	Modification
0.000	0.000	0.002	0.003	0.000	0.000	0.010	0.140	0.063	0.042	0.000	K63+Glycation
0.039	0.009	0.120	0.004	0.200	0.019	0.233	0.000	0.000	0.085	0.118	K102+Glycation
0.144	0.020	0.136	0.006	0.142	0.005	0.036	0.000	0.000	0.060	0.138	K137+Glycation
0.208	0.024	0.288	0.030	0.339	0.012	0.017	0.403	0.248	0.101	0.274	K148+Glycation
0.075	0.008	0.085	0.008	0.087	0.006	0.121	0.580	0.197	0.144	0.088	K168+Glycation
0.325	0.178	0.631	0.009	0.626	0.019	0.550	0.529	0.490	0.151	0.581	K182+Glycation
0.411	0.033	0.480	0.014	0.515	0.012	0.632	0.244	0.177	0.125	0.473	N301+A1G0
12.448	0.899	13.703	0.618	14.255	0.080	14.672	9.657	12.410	1.462	13.467	N301+A2G2F
5.141	0.373	5.476	0.186	6.166	0.148	4.852	4.088	5.777	0.642	5.458	N301+A1G1F
0.000	0.000	0.000	0.000	0.000	0.000	0.000	0.322	0.307	0.123	0.000	N301+A1S1F
0.703	0.050	0.776	0.035	0.796	0.029	0.928	0.895	0.880	0.080	0.781	N301+A2G0
30.052	2.351	28.838	1.471	28.667	0.971	26.689	30.825	29.838	1.652	29.229	N301+A2G0F
0.363	0.036	0.451	0.004	0.490	0.021	0.576	0.396	0.302	0.079	0.449	N301+A2G1
38.932	3.324	38.235	1.881	36.765	1.840	38.505	38.349	37.450	1.999	37.701	N301+A2G1F
1.386	0.055	1.496	0.067	1.435	0.047	0.714	1.093	0.739	0.288	1.404	N301+A2S1G1F
0.838	0.079	0.816	0.038	0.836	0.031	0.003	0.584	0.306	0.274	0.813	N301+A2S2F
0.278	0.005	0.302	0.030	0.291	0.030	0.268	0.000	0.000	0.114	0.274	N301+M4
0.753	0.068	0.994	0.104	0.966	0.088	0.577	0.728	0.489	0.188	0.847	N301+M5
96.850	0.066	96.802	0.208	96.946	0.486	96.788	97.655	97.886	0.428	96.815	Q1+Gln→Pyro-Glu
99.824	0.015	99.810	0.009	99.815	0.003	99.586	99.853	99.920	0.077	99.816	Q1+Gln→Pyro-Glu
1.348	0.537	1.685	0.036	1.778	0.045	0.673	3.083	2.684	0.667	1.735	G450+Lys
0.043	0.012	0.034	0.013	0.069	0.015	0.818	0.699	0.608	0.302	0.056	N33+Deamidation
0.334	0.069	0.778	0.054	1.213	0.027	1.545	3.159	2.233	0.842	1.014	~N136+Deamidation
0.035	0.008	0.132	0.004	0.219	0.004	0.321	0.823	0.734	0.261	0.175	~N137+Deamidation
0.034	0.005	0.070	0.037	0.115	0.020	0.343	0.879	1.399	0.428	0.103	N290+Deamidation
0.001	0.000	0.002	0.001	0.002	0.001	0.168	6.786	9.248	3.164	0.002	**N319+Deamidation**
0.368	0.038	0.747	0.019	1.257	0.045	1.951	0.738	1.314	0.486	0.757	N365+Deamidation
1.267	0.137	2.198	0.183	2.811	0.134	4.462	2.089	2.694	0.905	2.304	**N388+Deamidation**
2.177	0.040	2.211	0.125	2.522	0.059	0.065	0.000	0.001	1.043	2.200	M21+Oxidation
0.342	0.093	0.336	0.069	0.455	0.015	0.001	0.617	0.445	0.153	0.424	~M34+Oxidation
0.248	0.061	0.189	0.037	0.164	0.013	0.549	0.926	1.113	0.327	0.210	M81+Oxidation
3.654	0.683	2.560	0.348	2.435	0.152	3.556	25.225	29.209	9.505	3.064	W106+Oxidation
0.630	0.150	0.591	0.042	0.562	0.023	0.378	0.008	0.000	0.241	0.553	~W111+Oxidation
0.000	0.000	0.000	0.000	0.000	0.000	0.000	0.034	0.199	0.057	0.000	C133+Double Oxidation
0.000	0.000	0.000	0.000	0.000	0.000	0.000	0.011	0.179	0.051	0.000	C148+Double Oxidation
0.000	0.000	0.000	0.000	0.000	0.000	0.000	0.032	0.192	0.055	0.000	C193+Double Oxidation
2.673	0.158	2.843	0.254	2.686	0.243	1.820	2.215	2.407	0.344	2.578	M256+Oxidation
0.000	0.000	0.000	0.000	0.000	0.000	0.000	0.019	0.057	0.017	0.000	C265+Double Oxidation
0.016	0.004	0.021	0.002	0.033	0.002	0.068	0.000	0.000	0.018	0.020	C371+Double Oxidation
2.591	0.179	2.646	0.188	2.558	0.029	1.218	1.760	2.243	0.460	2.545	M432+Oxidation
0.000	0.000	0.000	0.000	0.001	0.001	0.000	2.192	0.000	0.633	0.000	~K38+Carbamylation
0.000	0.001	0.000	0.000	0.000	0.000	0.000	0.087	0.000	0.025	0.000	K38+Carbamylation
0.124	0.008	0.190	0.011	0.232	0.016	0.001	0.000	0.000	0.092	0.155	K102+Carbamylation
0.003	0.003	0.003	0.002	0.007	0.004	0.004	0.900	0.019	0.258	0.005	K278+Carbamylation
0.000	0.000	0.000	0.000	0.000	0.000	0.000	0.202	0.000	0.058	0.000	K321+Carbamylation
0.000	0.000	0.001	0.000	0.001	0.001	0.000	1.254	0.000	0.362	0.001	K338+Carbamylation

Table 3. Comparison of the oxidation, deamidation, and carbamylation modifications identified with the different digestion methods.

thermoscientific

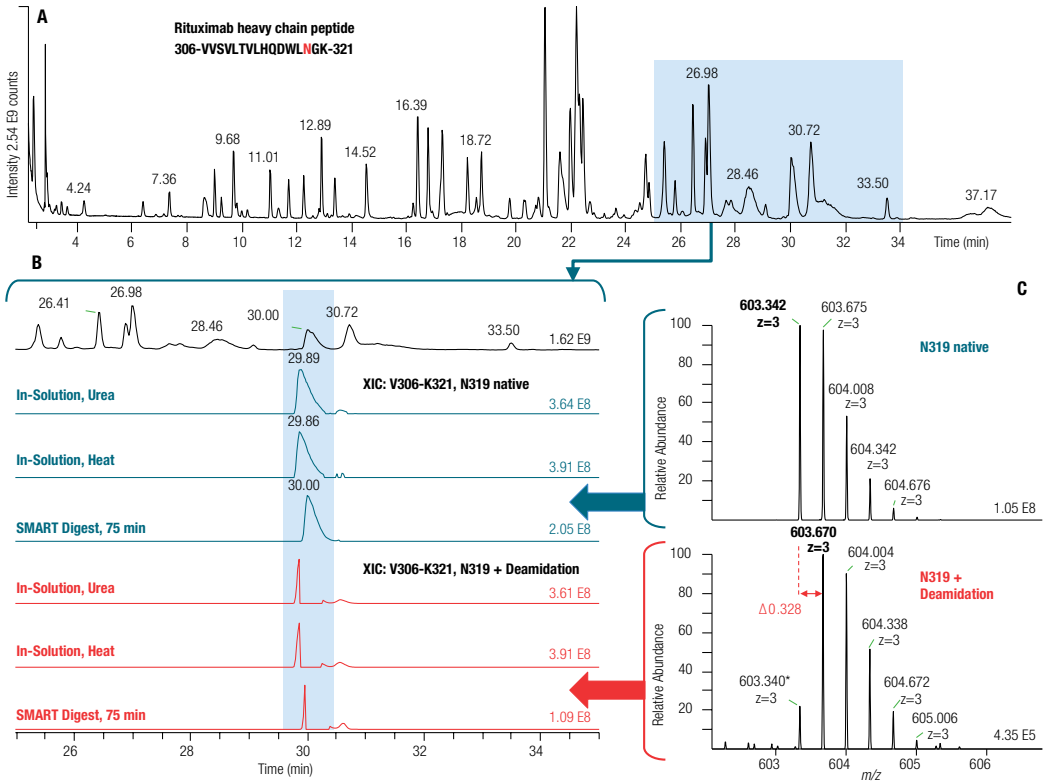

Figure 8. Total ion current chromatogram of the reduced SMART Digest sample, 75 min **(A)**, and extracted ion current chromatograms **(B)** for the peptide V306-K321 in the native and the deamidated form for the different runs. A comparison of the isotopic distributions of the $[M+3H]^{3+}$ ions **(C)** for the native and deamidated V306-K321 peptide.

methods. Overall, the extent of chemical modifications detected was similar for all digestion methods. The elevated temperatures during enzymatic digestion using the SMART Digest kit did not increase the amount of induced deamidation compared to in-solution-digested samples. In fact, the calculated deamidation (and oxidation) factors were lower or identical to the urea-treated samples, and heat-denaturation combined with in-solution digestion resulted in slightly increased modification levels. Optimization of the incubation time can be used to further minimize the introduction of chemical modification during digestion using the SMART Digest kit. For Rituximab,a digestion time of 15 min is feasible and results in complete sequence coverage and accurate relative quantification of PTMs. In contrast, prolonged digestion times >45 min can increase the amount of chemical modifications. Interestingly, some positions were more prone to undergo deamidation in one condition compared to the others, but no correlation with a specific digest condition was seen. Since the use of urea is omitted during the SMART Digest, lysine carbamylation was virtually absent in SMART Digest and urea-treated samples. This contributed to a less complex but comprehensive peptide map.

The huge time-saving potential, ease of use, and outstanding reproducibility of the SMART Digest make it the heart of a comprehensive peptide mapping workflow as applied in this study. When combined with the V anquish Flex UHPLC system, Orbitrap-based mass spectrometer, and the simple yet powerful tools within Chromeleon and BioPharma Finder software, SMART Digest kit facilitates standardized, fast, and reproducible peptide mapping workflows.

Description	Cat. No.
Thermo Scientific Acclaim VANQUISH C18, 2.2µm, 2.1 × 250mm	10043-322
Thermo Scientific SMART Digest Kit	10790-384

VWR COLLECTION

designed for your space

VWR® CONTOUR™ STYLE CABINET CONSTRUCTION

The Contour style of laboratory furniture features smooth, easy to maintain surfaces. The full-width extruded door and drawer pull becomes an integral element of each assembly. The heavy gauge steel full-frame construction has been specially engineered to withstand a full ton of pressure.

All Contour casework is manufactured of prime grade, cold rolled, U.S. Standard sheet steel with no ragged edges.

Warranty: One year beginning at the date of substantial completion that all products sold under contract shall be free from defect in materials and workmanship.

vwr.com/furniture

Cabinet Features

A. Flush Face Construction:
All doors and drawers are ¾" thick with radiused edges and full width integral pull.

B. Full Width Integral Pulls:
Radius edges on doors and drawer eliminates sharp corners.

C. One-Piece Drawer Body:
Radiused bottom for easy cleaning. Drawer head sound deadened for quiet operation. Weight capacity of drawer = 100 lbs.

D. Interchangeable Doors and Drawers

E. Full Extension Self-Closing Drawer:
Lock open feature allows drawer to stay open for loading and unloading. Drawer self-closes at 5". Nylon soft touch glides in the drawer. Slide channels provide 100 lbs. load-bearing capability.

F. Channel-Formed Back:
Constructed for maximum strength. Back is removable on cupboard units for access to pipe space.

G. Heavy Gauge Hinges:
Five-knuckle institutional type stainless steel hinges, nylon roller catches, and rubber door bumpers ensure quiet, secure closure. Hinges are non-corrosive to most acids and solvents.

H. Positive Latching Doors:
The doors are equipped with an exclusive positive latching mechanism. This locking mechanism ensures that the doors will self-close within the last few inches and prevents rebounding.

I. Rubber Door Bumpers:
For safe, quiet closures.

J. Leveling Bolt Access at all Four Corners:
Provides access for minor adjustments. Cabinet base features a die-formed gusset with a 3" long leveling bolt.

K. One-Piece Case Bottom and Front Rail:
Bottom is radiused at sides and rear for easy cleaning.

L. Completely Enclosed Toe Space:
Prevents dirt and bacteria from collecting in inaccessible areas, and prevents contamination in the laboratory.

M. Cupboards with Removable Rear Access Panels:
Allow for easy access to pipe chase area.

VWR Furniture | designed • delivered • installed

VWR COLLECTION

designed for your space

VWR® BENCH SELECTOR ONLINE DESIGN TOOL

The New VWR Bench Selector allows you to easily design a lab workstation complete with accessories. Follow four (4) easy steps — the configurator walks you through the simple process of selecting a VWR bench and adding accessories to build a lab workstation that best meets your needs. It has never been easier to design and get a quote on a lab workstation!

Visit **vwr.com/benchselector** today to discover a world of options!

For more information about VWR Furniture products and services, contact your VWR Furniture Specialist at **1.800.932.5000** or visit **vwr.com/furniture** today!

VWR Furniture | designed • delivered • installed

VWR COLLECTION

designed for every day use

VWR® CO_2 Resistant Tubes

For Protecting Samples Shipped on Dry Ice

- Keeps samples pH-stable
- Certified for shipping

VWR's CO_2 Resistant Tube is the only container closure system engineered to be CO_2 resistant and stop costly damage to molecular and cellular solutions when using dry ice. Made of durable, high-quality materials and fitted with an air-tight, secure-seal cap, VWR CO_2 Resistant Tubes form a protective barrier impermeable to CO_2, keeping the sample pH-stable when shipping or storing on dry ice.

Description	Package	Cat. No.	Pk/Cs
15mL CO_2 Resistant Tube, Non-Sterile	Sleeves of Ten	**10852-306**	**50/100**
15mL CO_2 Resistant Tube, Sterile	Sleeves of Ten	**10852-302**	**50/100**
50mL CO_2 Resistant Tube, Non-Sterile	Sleeves of Ten	**10852-308**	**50/100**
50mL CO_2 Resistant Tube, Sterile	Sleeves of Ten	**10852-304**	**50/100**

Azure Biosystems Presents the cSeries Imaging Systems for NIR, RGB, and Chemiluminescent Western Blot Applications

Azure Biosystems is dedicated to designing instruments that can deliver industry-leading performance across a broad range of laboratory applications, without overcomplicating the user experience.

We have designed a suite of upgradeable Western blot imaging systems that provides researchers industry-leading performance in a flexible system that allows them to use the best application for their research. Our instrument product line culminates in the c600 system (Figure 1), and is the only imaging line on the market that combines the following features:

- Infrared laser excitation for quantitative Western blot imaging in the near IR
- Picogram detection of proteins with chemiluminescent Westerns
- Versatile dye selection with Cy®5/Cy3/Cy2 excitation, and more
- Base unit fully upgrageable to the c600 system

Customers no longer have to choose one chemistry for their Western blots, they can buy one system and customize it to their needs.

Imaging in the Near IR

The popularity of near-infrared fluorescent (NIR) Western blot detection is due in part to the signal stability and low background offered by infrared fluorescent dyes, but more importantly to the additional questions you can ask with multiplex fluorescent detection. Azure Biosystem's cSeries laser technology offers two IR detection channels enabling a user to image more than one protein in an assay. Imaging with NIR dyes allows you to study multiple proteins in a blot, even if those proteins overlap in molecular weight.

Figure 1. Azure Biosystems c600 imager. The only system in the market able to image IR Western blots, RGB Western blots and chemiluminescent blots. IR, RGB, and Chemiluminescent Western all in one, upgradable, cutting edge system.

Because the secondary antibodies are imaged in two different channels, the resulting image can be spectrally separated for analysis (Figure 2). Additionally, you can use your second channel to easily probe for a loading control (Figure 3a). Our laser technology enables sensitivity that meets the performance of other laser systems (Figure 3b).

Sensitive Detection of Chemiluminescent Proteins

Chemiluminescence is still the most sensitive detection method for some assays. The Azure cSeries provides accurate and fast chemiluminescent detection, and the sensitivity, dynamic range, and linearity needed for quantatitative blot analysis. No matter what HRP substrate you are using, the Azure cSeries systems are compatible with your current protocol. Instead of using film and a developer, simply place your blot in the cSeries to get great results. Using high resolution cameras, and F 0.95 fast lens techonology, you can capture images with the same sensitivity as film (Figure 4a).

The biggest advantage to switching to digital imaging is the ability to get more

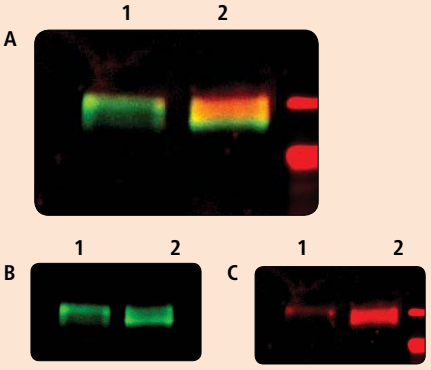

Figure 2. Simultaneous detection of EGFR and phospho-EGFR. Control cells (lane 1) and cells treated with EGF (lane 2) were imaged. EGFR was detected in the green channel (panel B), and phospho-EGFR was detected in the red channel (panel C). Panel A shows the green and red channels superimposed.

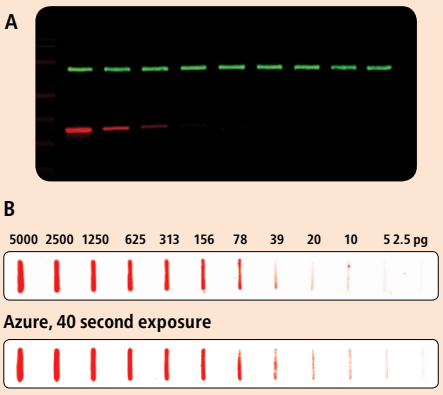

Figure 3. (a) Two color Western blot imaged with IR 700 and IR 800. **(b)** Azure performs equal to a competitor's laser scanner system, 7.5-times faster. A serial dilution of IR 700 antibody shows that the limit of detection is the same.

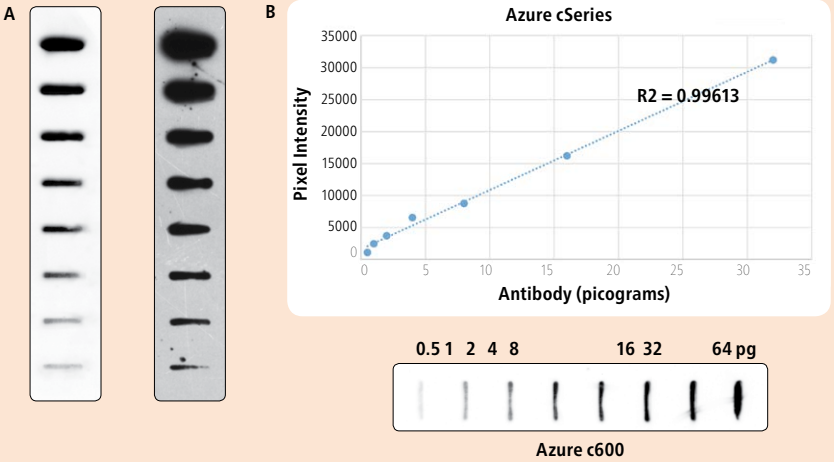

Figure 4. (a) Two slot blots of serially diluted HRP-coupled secondary antibodies were prepared on nitrocellulose. Both blots were treated with a substrate. Left: Imaged on the Azure cSeries for 2 minutes. Right: Imaged on film for 2 minutes. **(b)** Azure cSeries gives a linear response to a serial dilution of an HRP-coupled antibody.

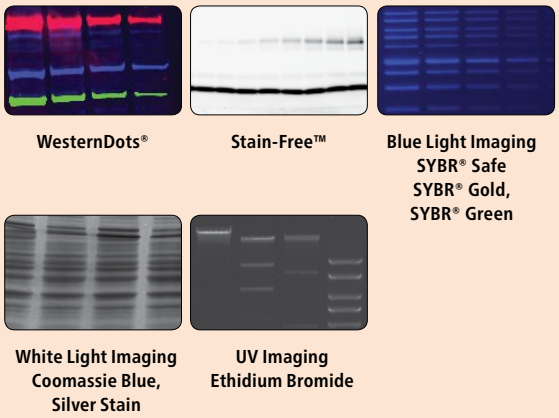

Figure 5. Application flexibility. The Azure c600 has eight different light sources and a seven position filter wheel, resulting in compatibility for the most critical dyes for protein work.

quantitative data from your Western blots. Film saturates quickly, making it difficult to quantify high-abundance proteins. The Azure cSeries has a broad dynamic range allowing quantitation over several orders of magnitude of protein concentration (Figure 4b).

Versatile Dye Selection

The Azure cSeries is not limited to just NIR and chemiluminescent Westerns. The Azure cSeries instruments can also be equipped with powerful LEDS for Cy™5/Cy3/Cy2 imaging or similar. The system also contains UV, white, and blue lights for imaging Ethidium bromide, Coomassie®, and Safe dyes. The cSeries is also able to image a wide range of dyes that have excitation maxima from 302nm to 785nm. This enables WesternDots™, Stain-Free™ gels and different types of in-gel fluorescence (Figure 5).

Azure cSeries

The Azure cSeries imagers are easy-to-use and reliable instruments for Western blot imaging, and enable labs to use one system for fluorescent and chemiluminescent Westerns. The simple user interface allows fast imaging of all sample types. Full upgradability means customers can have confidence that their system will grow and adapt with their needs.

Azure c600 Imaging System

Quantitative Westerns are Just the Beginning

- Three LEDs for Visible Fluorescent Imaging
- Two Lasers for NIR Fluorescent Imaging
- One Powerful System for Chemi, Visible, and NIR Fluorescent Imaging

The c600 is designed for the ultimate flexibility for Western blotting. Image chemiluminescent and fluorescent blots, as well as DNA and protein gels, in a small, compact, easy to use unit.

Description	Cat. No.	Unit
Azure c600 Imaging System	10147-214	Each

VWR bioMarke™

New Generation Size Exclusion Chromatography (SEC) Columns

Maximized resolution and optimized run time for small-scale preparative purification and analysis

Our new generation size exclusion chromatography columns called "Increase" are designed for high resolution in small-scale preparative purification and analysis for sample volumes up to 500µL. They deliver improved performance compared to predecessor columns:

- Reduced run time with maintained resolution for time saving or increased throughput
- Higher resolution for improved protein purity and analysis data
- Higher lot-to-lot consistency for better reproducibility

In 2017, GE expands the range of new generation SEC columns with Superdex™ 30 Increase

- Four choices of new generation SEC resins for small-scale preparative purification and analysis
  - Superdex 30 Increase is the replacement for Superdex Peptide columns

Superdex Superdex 30 Increase
Peptides and other small biomolecules
Fractionation range
Mr ~ 100 to 7,000

Superdex 200 Increase
mAb and other antibodies
Fractionation range
Mr ~ 10,000 to 600,000

Superdex 75 Increase
Recombinant tagged proteins
Fractionation range
Mr ~ 3,000 to 70,000

Superose™ 6 Increase
Larger proteins and protein complexes
Fractionation range
Mr ~ 5,000 to 5,000,000

Distributor
GE Healthcare

New generation SEC columns deliver improved performance compared to predecessor columns

The agarose resins have been optimized to deliver improved performance compared with their predecessors (smaller and more rigid beads, narrower particle size distribution, higher selectivity).

Higher resolution at the same flow rate

Faster separation with the same resolution

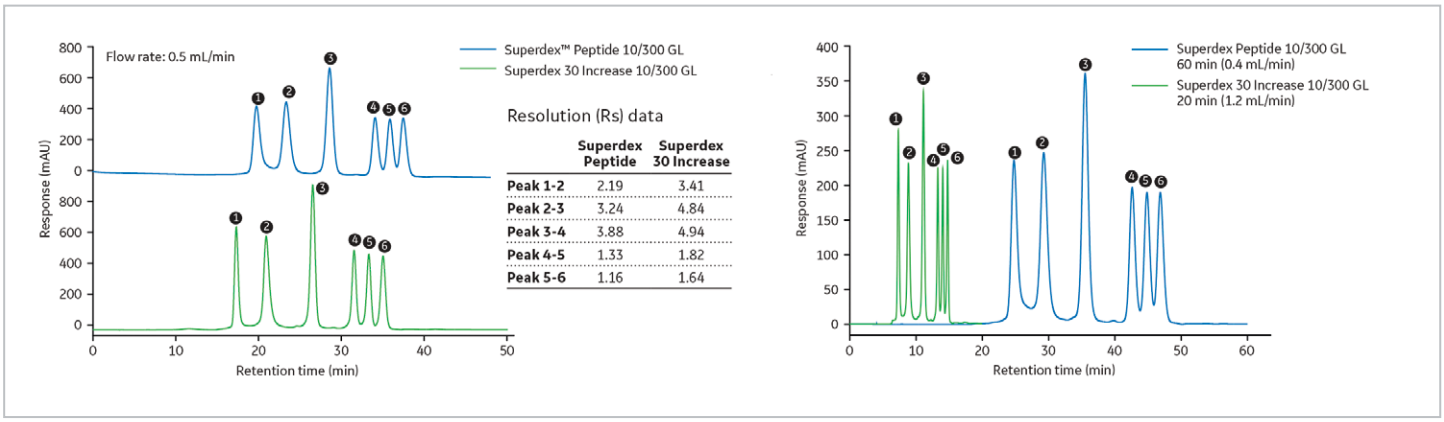

Fig 1. Compared with Superdex Peptide, new generation Superdex 30 Increase delivers up to 50% higher resolution at the same flow rate, or three times faster separation with the same resolution.

Three column dimensions for new generation SEC columns to fit different needs

10mm × 300mm (Tricorn™ 10/300 GL)

- High resolution analysis (25–500µL sample volume)
- Small-scale preparative runs (milligram amount)

3.2mm × 300mm (Precision Column 3.2/300)

- High resolution analysis (4–50µL sample volume)
- Small-scale preparative runs (microgram [µg] amount)
- Low sample and buffer Consumption

5mm × 150mm (Tricorn 5/150)

- Purity check
- Rapid screening
- Low sample (4–50µL sample volume) and buffer consumption

These columns are recommended for use with ÄKTA™ pure 25 systems and traditional HPLC systems. Transparency of the columns enable an easy inspection of the resin bed.

US ONLY

Ordering Information

Description	Dimension, mm	Cat. No.	Qty
Superdex 30 Increase*	10 × 300	**76015-026**	**Each**
Superdex 30 Increase*	3.2 × 300	**76015-028**	**Each**
Superdex 200 Increase	10 × 300	**89497-272**	**Each**
Superdex 200 Increase	3.2 × 300	**89497-276**	**Each**
Superdex 200 Increase	5 x 150	**89497-274**	**Each**

** These products are not available in Canada. Please contact your VWR Sales Rep to learn about easy access to similar options in your region.*

Common Mistakes When Using a Laboratory Freeze Dryer

By Kelly Williams, Product Manager, Labconco

Labconco offers these solutions to common mistakes made in laboratory lyophilization. Following these suggestions can increase the quality of your samples and prolong the life of your freeze dryer.

Adequate vacuum levels and collector temperatures are required to keep samples frozen during primary drying.

INCOMPATIBLE SAMPLES

Often a sample is placed on a freeze dryer without any consideration as to the compatibility of the sample with the specifications of the freeze dryer. When lyophilizing, it is important to identify the components of the sample and their requirements for lyophilization. Incompatibility can result in decreased quality of the freeze dried sample and, more importantly, expensive damage to the freeze dryer or vacuum pump.

Collector Temperature

Although it is not critical to know the precise freezing point of a sample, estimating the general freezing point or eutectic temperature of your sample is important. The collector temperature of the freeze dryer is recommended to be 15°C to 20°C below the freezing point of a sample. This difference is necessary to keep the sample frozen during primary drying and to effectively trap the lyophilized vapors before they reach the vacuum pump. Collectors have fixed temperatures at -50°C, -84°C, and -105°C. For aqueous samples, a -50°C collector temperature is adequate. When solvents are present in samples, the freezing point is suppressed. For samples containing acetonitrile, a -84°C collector is recommended and for samples with up to 10% methanol, a -105°C collector is recommended. No harm is caused by using a freeze dryer with a collector that is colder than the minimum requirement.

Collector Size

It is important to ensure the size of the collector is big enough to accommodate the volume of the entire sample load. Stopping a run and defrosting the collector is not an ideal option. It is easier to make sure your entire run can be accommodated before starting the run. No harm is caused by using a collector that is bigger than the minimum size requirement.

Component Compatibility

Some samples may contain compounds that require special components in the freeze dry system. Acids, solvents, and particulates are common compounds that can be accommodated with modifications.

Acids	Polytetrafluroethylene (PTFE) coatings protect stainless steel collectors and coils
Solvents	Glass lids are used when a solvent damages acrylic lids
Particulates	Inline HEPA filters, placed between the collector and the vacuum pump, protect vacuum pumps from damage from particulates

VACUUM PUMP DAMAGE

Maintaining deep vacuum levels is the most common problem in laboratory freeze drying. A damaged vacuum pump is the leading cause of inadequate vacuum levels in a freeze dry system. If the

vapors are not completely collected on the coils in the collector, they will enter the vacuum pump. Oil vacuum pumps are the most susceptible to damage from these vapors. Often the vapors will condense in the pump and mix with the oil. Once mixed in the oil, water can cause extensive damage to a pump while solvents and acids can cause even more damage. Combination rotary vane/diaphragm and scroll pumps are more resistant to harmful vapors but still can be damaged from exposure.

Damage to any pump will be avoided by preventing vapors from entering the pump. Ensuring the compatibility of the samples to the freeze dryer, as discussed earlier, is the most important preventative step to vapors entering the pump. Here are more suggestions.

Start-Up Sequence

To prevent vapors from entering the pump, make sure the collector coils have cooled to at least -40°C before the vacuum pump is started. If the collector coils are not at adequate temperatures, they will not trap moisture from the air and any volatile vapors during system pull down. Having a purge valve that allows the vacuum pump oil to heat up before system pull down will prevent vapors from condensing in the hot oil.

Shut Down

The majority of vacuum pumps have a gas ballast that can be used to purge containments from pump oil. After the freeze dry run, a pump should be allowed to operate with the gas ballast open for 20–30 minutes. This gives any vapors that condensed in the pump an opening in which to leave the pump. Running the pump heats the oil so that the contaminants are essentially distilled out of the oil.

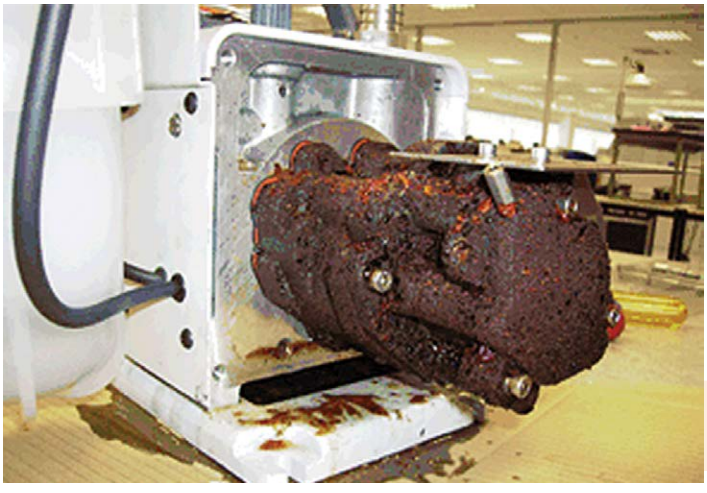

Vacuum pump damage can be extensive and costly, like the pump shown to the left.

Collectors with exposed coils outperform smooth-walled collectors in vapor load tests.

Maintenance

Frequent oil changes will limit the damage to the pump if vapors enter the pump. During oil changes, flushing fluid can be used to rinse away any contaminates within the vacuum pump. It is important that oil levels are maintained and pumps are never allowed to run above or below the recommended oil levels.

FREEZE DRYER MAINTENANCE

Freeze dryers are often laboratory workhorses that are simply used for years with little attention to their maintenance needs (aside from vacuum pump oil changes) until one day they no longer work. With very little effort, the lifespan of a freeze dryer can be greatly increased.

Emptying the Collector

At the end of a run, it is very easy to take the finished lyophilized sample and forget about defrosting and emptying the ice in the collector. Limiting the exposure of water or even worse, acids and solvents, to the freeze dryer will lengthen its lifespan. Freeze dry collectors should be defrosted, drained, and wiped down immediately after every use. Neutralizing collector coils after any acid exposure is critical. If the collector is not drained, and the liquid is not noticed before the next start up, collector liquid will be pulled into the vacuum pump. Some freeze dryers feature drain line detectors to prevent this maintenance nightmare from occurring.

LABCONCO

Checking Lids for Crazing

With extended exposure to some solvents, like acetonitrile, over time, acrylic can craze. Lid crazing can compromise vacuum levels and if allowed to continue, may cause the lid to implode when exposed to deep vacuums. Replacing the lid with visible crazing or using a glass lid when lyophilizing incompatible solvents will eliminate freeze dryer downtime.

These common mistakes are often eliminated in newer freeze dryers as their designs offer many features that make freeze drying and freeze dryer maintenance easier. Features such as remote notification of operating and maintenance alerts, one-button data logging, auto start-up, and onboard diagnostics are just a few of the features available for labs that want a hassle-free lyophilizer that will provide high quality results for decades.

Accessories can make lyophilizing easier. New End-Zone™ End Point Detection sends a notification when lyophilization is complete.

Description	Cat. No.	Unit
FreeZone® Benchtop Freeze Dryer, 2.5L, -50°C	75999-778	Each
FreeZone Benchtop Freeze Dryer, 4.5L, -84°C	75999-822	Each
FreeZone Benchtop Freeze Dryer, 4.5L, -105°C	76000-648	Each
FreeZone Benchtop Freeze Dryer, 8L, -50°C	76000-508	Each
FreeZone Console Freeze Dryer, 6L, -84°C	76000-524	Each
FreeZone Console Freeze Dryer, 12L, -50°C	76000-010	Each
FreeZone Console Freeze Dryer, 18L, -50°C	76000-552	Each
End-Zone™ Starter Kit	76000-968	Each

BD Peptone Preview Pak

BD

Are You Feeding Your Cells What They Need to Get Your Desired Results?

- Easy-to-test, animal-free peptone packs
- Supplements provide different and unique nutritional profiles to help optmize your cell culture process
- May be used to optimize and enhance mammalian and microbial applications

BD has taken its years of expertise in developing high quality cell culture supplements and feeds to design new peptones from a variety of different biological sources. The BD Peptone Preview Pak — featuring our new pea, wheat, cotton, soy, and yeast peptones — provides unique nutritional profiles compared to other current cell culture supplements in the market today.

Description	Cat. No.	Unit
BD Peptone Preview Pak	75878-702	Pack of 6
BD Wheat 100 UF	75878-704	Each
BD Cotton 100 UF	75878-706	Each
BD Cotton 200 UF	75878-708	Each
BD Soy 100	75878-710	Each
BD Yeast 100	75878-410	Each
BD Pea 100 UF	75878-412	Each

Mesenchymal Stem Cell and Media System

PromoCell

Reliable Results for Your Research

- **Defined Cells.** Each Mesenchymal Stem Cell (MSC) batch is tested in accordance with ISCT* recommendations for CD73+/CD90+/CD105+ and CD14-/CD19-/CD34-/CD45-/HLA-DR
- **Guaranteed Performance.** Each of our MSC lots is guaranteed to grow with a doubling time of <30h through at least 10 population doublings and is also tested for differentiation into osteoblasts, adipocytes, and chondrocytes
- **Complimentary Research Tools.** PromoCell offers a comprehensive portfolio of cell biology research products including Growth & Differentiation Factors, Stem Cell Fate Regulators, Antibodies & ELISAs, Cellular Analysis, and Cell Transfection

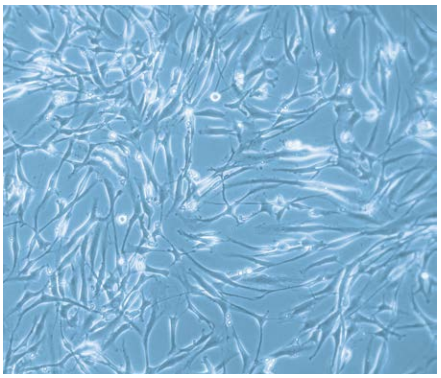

PromoCell is a premier manufacturer of cell culture products with a complete portfolio featuring human Mesenchymal Stem Cell (hMSC) culture media, growth media, and differentiation media. All of our hMSC are isolated in accordance to the highest ethical standards and extensively quality tested including marker characterization, growth performance, and *in vitro* differentiation in our media.

* ISCT (International Society for Cellular Therapy) Cytotherapy (2006) Vol. 8, No. 4, 315-317

Description	Size	Cat. No.	Unit
Human Mesenchymal Stem Cells			
MSC from Bone Marrow (hMSC-BM)	500.000 cryopreserved cells	**10172-152**	**Each**
MSC from Umbilical Cord Matrix (hMSC-UC)	500.000 cryopreserved cells	**10172-148**	**Each**
MSC from Adipose Tissue (hMSC-AT)	500.000 cryopreserved cells	**10172-156**	**Each**
Mesenchymal Growth Media			
MSC Growth Medium 2 (Serum Containing)	500 mL	**75812-652**	**Each**
MSC Growth Medium DXF (Defined & Xeno-Free)	500 mL	**10172-384**	**Each**
Mesenchymal Stem Cell (MSC) Differentiation Media			
MSC Adipogenic Differentiation Medium 2	100 mL	**75812-654**	**Each**
MSC Osteogenic Differentiation Medium	100 mL	**10172-378**	**Each**
MSC Chondrogenic Differentiation Medium	100 mL	**10172-376**	**Each**

Take the 20 Minute Route to Mycoplasma Detection

Lonza

Get Reliable Results within 20 Minutes Using the Lonza MycoAlert™ PLUS Assay

- Bioluminescence-based technology with no DNA extraction necessary
- Simply add two reagents to the culture supernatant and perform two luminescence readings
- Detects all common mollicute contaminations, except Ureaplasma (Mycoplasma, Acholeplasma, Entomoplasma, and Spiroplasma)

The MycoAlert PLUS Assay is a selective biochemical test that exploits the activity of mycoplasm enzymes, which are not present in eukaryotic cells. If viable mycoplasma are present, the enzyn react with the MycoAlert PLUS Substrate and generate ATP. The ATP is then transferred into a li signal via the luciferase enzyme in the MycoAlert PLUS Reagent to show that mycoplasma is pr ent. The MycoAlert Assay Control Set (does NOT contain mycoplasma) is sold separately.

Visit vwr.com/lonzamycoalert for more information!

Description	Size	Cat. No.	Unit
MycoAlert™ Plus Mycoplasma Detection Kit	10 Tests	**75860-358**	**Each**
MycoAlert™ Plus Mycoplasma Detection Kit	30 Tests	**75860-360**	**Each**
MycoAlert™ Plus Mycoplasma Detection Kit	50 Tests	**75860-362**	**Each**
MycoAlert™ Plus Mycoplasma Detection Kit	100 Tests	**75866-212**	**Each**
MycoAlert™ Assay Control Set	10 Tests	**75870-450**	**Each**

Enhanced, Non-Viral Gene Delivery to Stem Cells with jetMESSENGER™ mRNA Transfection Reagent

INTRODUCTION

Growing interest in stem cells as a unique cellular system is driven by their self-renewal capacity and immune suppressive properties, as well as the potential to differentiate into various cell types. Many studies have already demonstrated the promising future of stem cells in developmental biology, regenerative medicine, and disease therapy[1]. Hence, developing an efficient gene transfer method to modulate gene expression has become indispensable to further understand the molecular function of single genes in stem cells, such as mesenchymal stem cells (hMSC)[2].

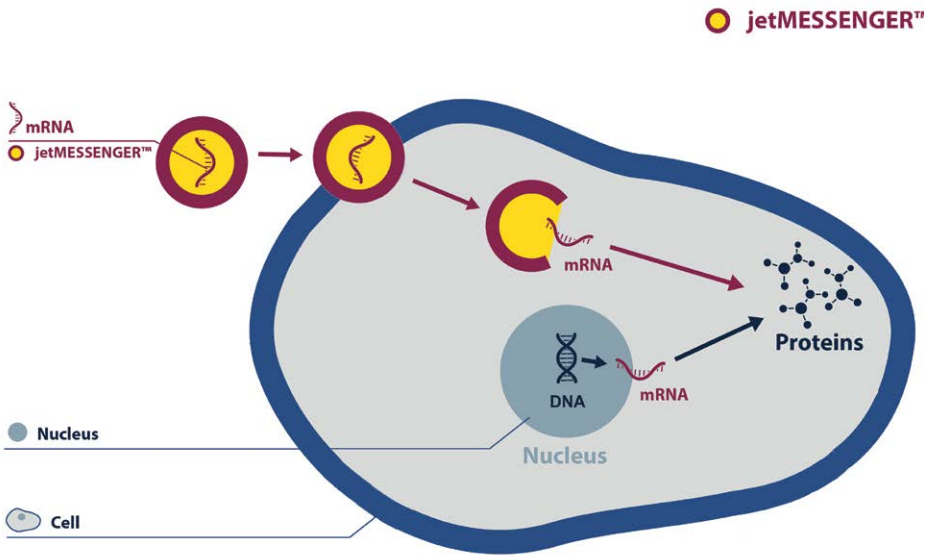

As an alternative to viral-based transfection methods, which give rise to potential pathogenicity and immune response risks, we have developed an efficient, non-viral mRNA transfection reagent — jetMESSENGER — that leads to outstanding transfection efficiencies in both embryonic and adult stem cells. The success of mRNA delivery using jetMESSENGER is mainly due to circumventing the need for nuclear import of DNA, hindered in difficult-to-transfect cells mainly by their slow-to-none dividing rates[3].

MATERIAL & METHODS

hMSC were purchased from Lonza and maintained in Mesenchymal Stem Cell Growth Medium (MSCBM™) and supplemented with Lonza MSCGM SingleQuots™. Mouse embryonic stem cells (mES) were purchased from MilliporeSigma (Pluristem 129S6 mES), grown on cell culture dishes coated with 0.1% gelatin (Greiner Bio-One), and cultured in DMEM with glucose 4.5g/L supplemented with L-Glutamine 1%, non-essential amino acids 1%, HEPES 1%, penicillin-streptomycin 1%, ESGRO® (mLIF) ESG1107 at 0.01%, ESG1106 0.1%, and MTG (Sigma-Aldrich® M6145) at 13.6µL per liter of medium. For transfection experiments, hMSC were seeded at 3 x 10^3 cells per well of 96-well plates or at 1.2 x 10^4 cells per well of 24-well plates in complete medium three days before transfection. On the day of transfection, jetMESSENGER/EGFP mRNA, Lipofectamine® 2000 (L2K)/EGFP, and Lipofectamine 3000 (L3K)/EGFP plasmid DNA complexes were prepared according to the manufacturers' recommendations for each reagent. Briefly, transfection with jetMESSENGER was performed as described: 100-150ng (per well of 96-well plate) or 400-500ng of EGFP-encoding mRNA (per well of 24-well plate) were first diluted in the provided mRNA buffer, followed by the mixing-in of respectively 0.4-0.5µL and 0.8-1.2µL jetMESSENGER. Following an incubation of 15 minutes at room temperature, jetMESSENGER complexes were simply added dropwise to cells in their complete growth medium.

For transfection experiments, mES were seeded at 5 x 10^4 cells per well of 24-well plates in complete medium three days before transfection. On the day of transfection, jetMESSENGER/EGFP mRNA, L2K/EGFP, and L3K/EGFP plasmid DNA complexes were prepared according to the manufacturers' recommendations for each reagent. Transfection with jetMESSENGER was performed with 400–600ng of mRNA of interest pre-diluted in the provided mRNA buffer, followed by the mixing-in of 0.8–1.4µL jetMESSENGER. Transfection efficiency was assessed 24 hours post-transfection by FACS and fluorescence microscopy analysis of EGFP positively expressing cells.

RESULTS & CONCLUSION

Here, we demonstrate that with jetMESSENGER, mRNA transfection reagent manufactured at Polyplus-transfection®, transfection efficiencies obtained in hMSC and mES cells were respectively superior to 90% and to 50% (Figure 1). Remarkably, in comparison to the competitor's DNA

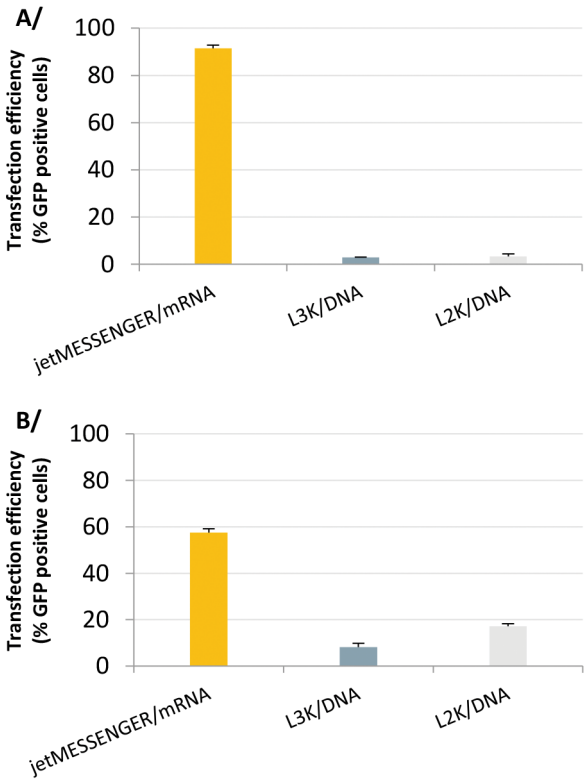

Figure 1. jetMESSENGER achieves outstanding transfection efficiencies in comparison to the main DNA transfection reagents in hMSC and mES cells. Transfection efficiency was assessed by FACS analysis in hMSC (A/) and mES cells (B/) 24 h after transfection with jetMESSENGER/EGFP mRNA or the competitor's DNA transfection reagents L2K and L3K/pCMV-EGFP plasmid. Conditions were set according to the manufacturers' recommendation.

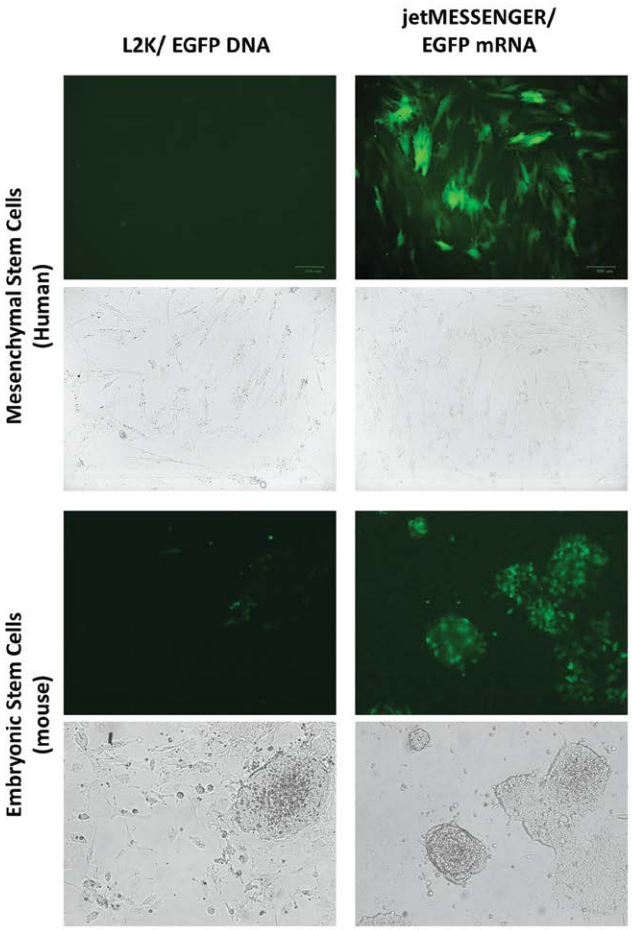

Figure 2. jetMESSENGER leads to high transfection efficiency in hMSC and mES colonies, along with higher cell viability. hMSC and mES cells were analyzed 24 h post-transfection using fluorescent microscopy and phase contrast. Transfections were performed with jetMESSENGER/EGFP mRNA and the competitor's DNA transfection reagents L2K/pCMV-EGFP according to the manufacturers' recommendations for each reagent. Data is representative of cells observed 24h post-transfection.

transfection reagents, jetMESSENGER mRNA transfection reagent led to a 50-fold increase in hMSC and to a 10-fold increase in the number of positively EGFP expressing mES cells.

As further illustrated by fluorescence microscopy, hMSC and mES cells transfected with jetMESSENGER/EGFP mRNA demonstrated a high transfection efficiency in comparison to the competitor's DNA transfection reagent L2K, while maintaining their cell morphology. In the case of mES cells, they retained their ability to form colonies of different sizes in 2D culture models (Figure 2).

Therefore, in addition to being a simple and ready-to-use transfection reagent that leads to outstanding transfection efficiencies in known to be hard-to-transfect stem cells, the jetMESSENGER delivery mechanism is gentle and consequently maintains a high cellular viability and physiologically relevant morphology.

US ONLY

Product	Reagent Size	Buffer Size	Cat. No.
jetMESSENGER™	0.1 mL	10 mL	75806-306
	0.75 mL	60 mL	75806-224
	1.5 mL	2 x 60 mL	75806-226

These products are not available in Canada. Please contact your VWR Sales Rep to learn about easy access to similar options in your region.

Sample Storage Tubes as Quality-Critical Components in Biobanking

Biobanks store biological samples and associated data to make them available for clinical studies as well as research on biomarkers, personalized medicine, and public health. The paramount goal of biobanking is the preservation of sample integrity during all steps of sample collection, processing, storage, and delivery; hence, factors influencing the sample quality during these steps need to be understood and controlled.

Whereas storage temperatures and environments as well as methods for secure sample tracking were always considered important factors in biobanking, the actual sample containing tubes have long been disregarded. Here we emphasize the importance of sample tubes as critical components of biobanking. In particular, Cryo.s™ Biobanking Tubes are analyzed with regards to cleanliness of tube raw material, tube closure, biomolecule adsorption onto the tube surface, and quality of the datamatrix barcodes used for tube identification and tracking.

POLYMER QUALITY AND LEACHABLES

Background

Multiple additives and agents can be utilized to alter the physical properties and processability of polymers used for labware production. Such chemicals are:

- UV stabilizers (e.g. benzophenone, benzotriazole, oxalanilide)
- antioxidants (e.g. organo phosphites)
- thermo stabilizers
- nucleation starters
- plasticisers (e.g., phthalate esters)
- mold release agents
- antistatic agents
- irradiation protectors
- clarifiers

Several studies have shown that polymer additives or their degradation products can migrate out of polymer-based microtiter plates or tubes and affect the outcome of biochemical assays performed with these products.

Virtually all polymer-based cryogenic storage tubes are made of polypropylene — a polymer proven to be excellently suited for the application at ultra-low temperatures. Today, an immense variety of different polypropylene qualities are available, although these raw materials widely differ in chemical composition and physical properties, as well as purity and certification.

Greiner Bio-One uses a medical grade, USP class VI certified polypropylene type for

greiner bio-one

Manufacturer Code	Tube Code	Extraction and IR Spectrum to Check for Amide	Extraction and Complete GC/MS Scan
Greiner Bio-One	G1 (300 µL Cryo.s™ Biobanking Tubes, non-sterile)	•	•
A	A1	•	-
B	B1	•	-
C	C1	•	-
D	D1	•	-
	D2	•	-

Table 1: 96-way cryogenic storage tubes from different suppliers were tested for leachables. This table provides an overview on leachable tests performed with selected tubes from Greiner Bio-One and other suppliers. Besides Greiner Bio-One, all other tube manufacturers are anonymized and tube codes are utilized to differentiate between different tube types offered by individual manufacturers (e.g., manufacturer 'D' offers the two different tube types 'D1' and 'D2').

the production of all Cryo.s Biobanking Tubes. In this context, the attribute 'medical grade' refers to the comprehensive certification of the material (e.g., European Pharmacopeia 3.1.3, 3.1.6 and 3.2.2), special cleaning processes before production start, and more than 15 years of history of the raw material with unchanged polymer composition. The USP class VI certification refers to a biocompatibility testing in accordance with the United States Pharmacopeia (USP). Primarily, passing this test is indicative of a high biocompatibility of the tested raw material; secondarily, it suggests a low content of leachables in the material. In addition, the raw material of Cryo.s Biobanking Tubes is certified free of the following chemical elements and agents:[1]

- heavy metals
- phthalate esters
- mold release agents
- antistatic agents
- TSE and BSE

Method

In order to assess the potential contaminations of storage tubes with amides (often used as mold release agents in injection molding), six different cryogenic storage tubes (see Table 1) were extracted with 50% ethanol in water for nine days at room temperature. Subsequently, the extractable material was characterized by IR spectroscopy after complete evaporation of the solvent. Typically amides yield signals in the infrared wave bands between 1630 and 1690cm-1 (C=O stretch) and between 3300 and 3700cm-1 (N-H stretch). In a second leachable test, Greiner Bio-One's Cryo.s Biobanking Tubes (300µL version, non-sterile version) were extracted with four different solvents: 10% ethanol/water, acetic acidacetate- buffer (pH 4.6), Tris-EDTA-buffer (pH 8.0) and 100% DMSO. This extraction was carried out over 72h at 37°C. Subsequently complete GC/MS fingerprints were recorded. This analysis was performed by UL International GmbH (Ochsenhausen, Germany).

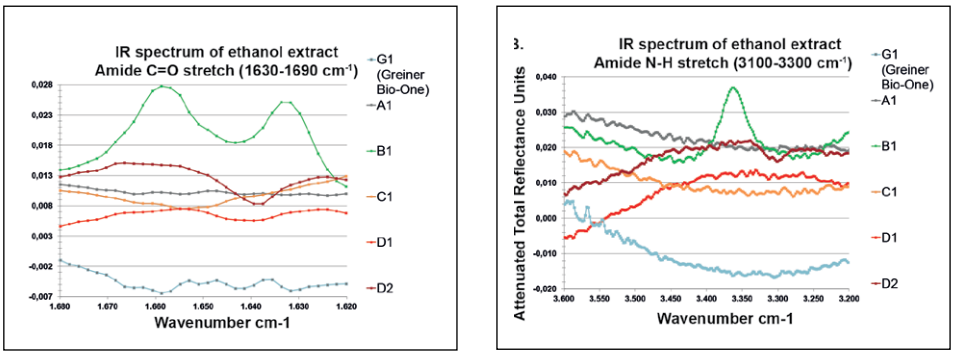

Figure 1. Extraction of cryogenic tubes with 50% ethanol in water with subsequent IR-spectroscopical analysis revealed amide-specific signals in the extract from tube 'B1' and mild signals in the extracts from tubes 'D1' and 'D2'. **A:** IR spectrum from 1620-1690cm-1. **B:** IR spectrum from 3220-3600cm-1.

Results

The IR spectra of ethanol extracts indicated the potential contamination of tube type 'B1' from manufacturer 'B' with amides. A mild contamination with amides was also detectable for the tubes 'D1' and 'D2' from manufacturer 'D'. All other tube extracts did not reveal amide-specific peaks in their IR spectra (Figure 1). The full GC/MS footprint of four different extracts (Figure 2A. ethanol/water; Figure 2B. Tris-EDTA-buffer, pH 8.0; Figure 2C Acetic acid-acetate-buffer, pH 4.6; Figure 2D. 100 % DMSO) of Greiner Bio-One's Cryo.s Biobanking Tubes revealed no extracted substances in any of the four extracts to undermine the high purity of the raw materials used for producing these tubes.

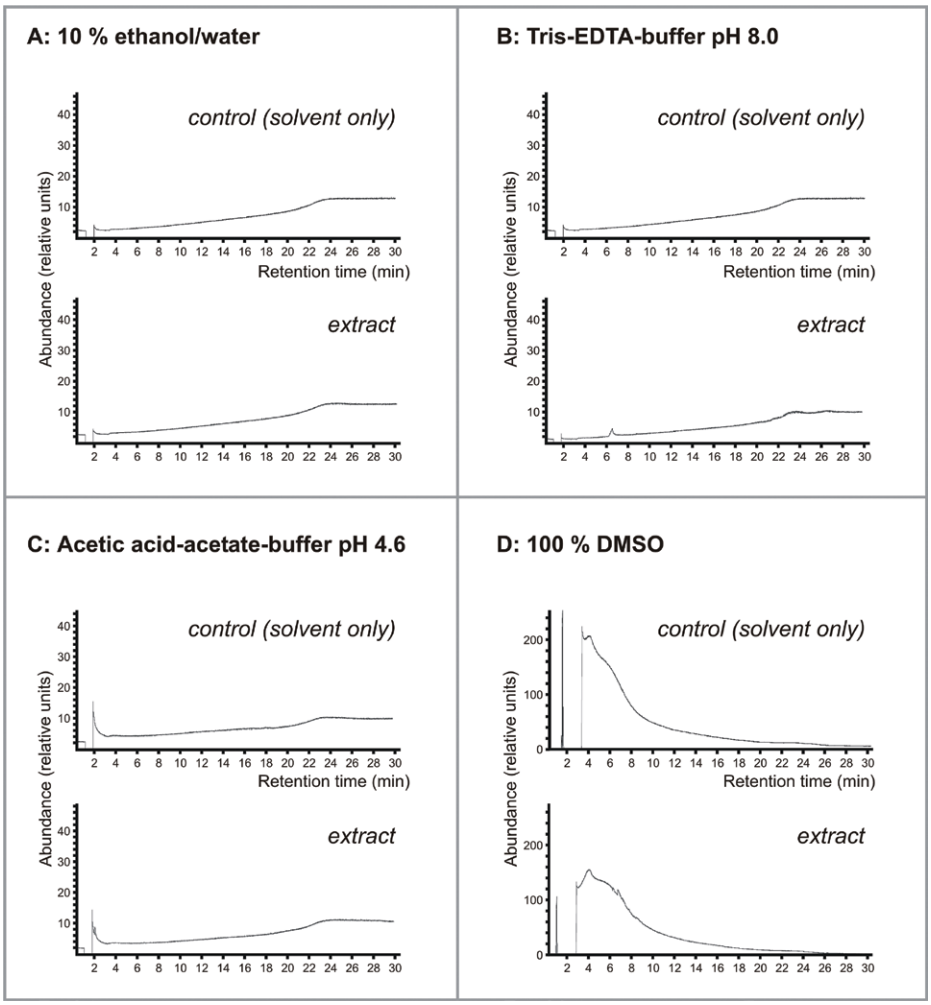

Figure 2. Extraction of Cryo.s Biobanking Tubes with four different solvents and subsequent GC/MS footprint analysis of the extracts. Extraction with 10% ethanol/water **(A)**, basic buffer solution (Tris-EDTA-buffer pH 8.0, **B),** acidic buffer solution (Acetic acid-acetate-buffer pH 4.6, **C)** and 100% DMSO **(D)** revealed no significant extractable substances.

Conclusion

Greiner Bio-One utilizes a high-quality, virgin and pure polypropylene type for the production of Cryo.s Biobanking Tubes. Extraction of these tubes with four different solvents revealed no detectable substances in the corresponding GC/MS fingerprints. Exemplified based on the presence of amide-specific IR signals in ethanolic extracts from some tube types, it becomes evident that the absence of leachable additives is not a guaranteed feature of tubes intended for sample storage in biobanking. Rather, raw material types vary between individual tube manufacturers and commonly accepted standards, such as the use of materials with low additive content, are still missing.

BIOMOLECULE ADSORPTION ONTO STORAGE TUBE SURFACES

Background

In biobanking, the concentration of biomarkers in liquid samples (e.g., blood serum) should remain unchanged over the entire period of sample processing and storage. However, there is a general risk of certain biomarkers binding onto the surfaces of tubes used for sample aliquotation and storage. Such unintended sample adsorption onto tube surfaces depends on the actual type of biomolecule (e.g., nucleic acid, polysaccharide, lipid, peptide, protein, etc.), as well as the type of tube raw material[iv] and details of the tube manufacturing process. In order to assess the adsorption of biomolecules onto storage tube surfaces, we have chosen an Iodine125-labelled derivative of the peptide Insulin-like growth factor 1 (IGF 1I125) as the test substance and developed a radioactivity-based adsorption assay (Figure 3).

Method

Humane IGF 1 was labelled with I125 on tyrosine residues applying the lactoperoxidase method, purified by HPLC (Dr. Carsten Tober, rent-a-lab, Reutlingen/Germany) and dissolved in fetal calf serum (FCS) to yield an IGF 1I125 concentration of 33.3ng/mL. Disc-shaped material samples (Ø = 5.2mm) were punched out of the side walls (Figure 3A) of cryogenic storage tubes from different suppliers (Table 2). Three tubes were analyzed per suppiler. The discs were placed into the wells of 6-well plates. The internal side of each material sample (originally facing towards the tube's interior) was incubated with 30µL test solution overnight at -80°C (Figure 3B). After incubation, the test solution was completely removed and the material samples were put into the wells of a 96-well plate with scintillation fluid. Emitted gamma-radiation was quantified and adsorbed IGF 1I125 determined based on standard curves derived from known amounts of IGF 1I125 (Figure 3C).

Results

The two tested sterile tube versions 'G2' and 'D1' revealed higher IGF 1I125 adsorption than the tested non-sterile tube types 'A1', 'G1', 'B1' and 'C1' (Figure

greiner bio-one

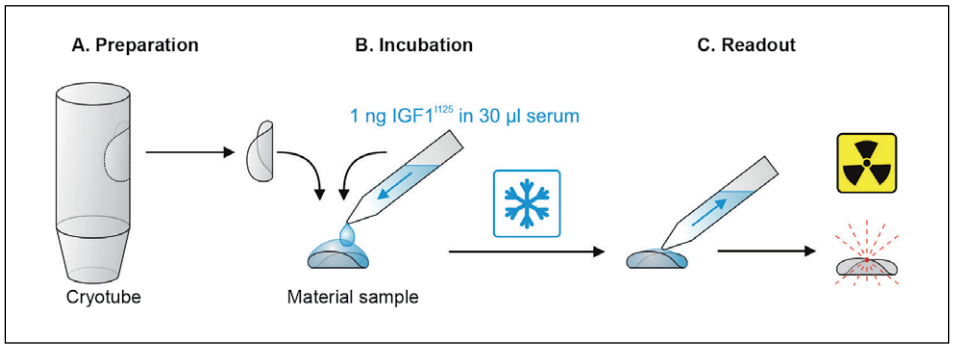

Figure 3. Experimental procedure of the adsorption assays with materia lsample preparation **(A)** material sample incubation with radioactively labelled test substance IGF 1I125 in serum, -80 °C, **B)** and quantification of emitted radiation from adsorbed IGF 1I125 **(C).**

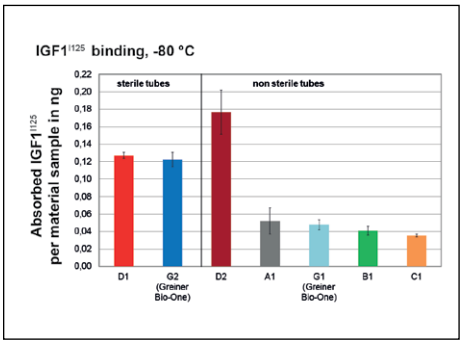

Figure 4. Amount of IGF 1I125 adsorbed onto material samples (5.2mm-discs) after incubation at -80°C with 30µL FCS containing a total of 1ng IGF 1I125. Error bars indicate standard errors of the mean (n=3).

4). Whereas 'G2' and 'D1' adsorbed about 12% of the IGF 1I125 present in the serum sample used for incubation, the non-sterile tube types 'A1', 'G1', 'B1' and 'C1' adsorbed only 3.5–5% of the contained IGF 1I125. One non-sterile tube type, namely tube 'D2', revealed a >4 times higher adsorption than the average of all other tested non-sterile tubes. With this tube an absorption rate of 17.5% of the present IGF 1I125 was observed.

Conclusion

Irradiation-based procedures regularly used for the sterilization of cryogenic storage tubes bear the potential risk of introducing unwanted binding sites for biomolecules which then may be adsorbed onto the product surface.

The IGF 1I125 adsorption assay presented here indeed indicates higher IGF 1I125 binding onto sterile tube versions (Greiner Bio-One and manufacturer 'D') as compared to the average non-sterile tube. Although non-sterile tubes may be regarded as a gold standard for liquid sample storage, one non-sterile tube (tube 'D2') from manufacturer 'D' yielded above-average IGF 1I125 adsorption at -80°C.

The data shown here indicate differences in IGF 1I125 adsorption onto tube surfaces depending on the tube type and sterilization. It is likely that other classes of biomolecules reveal adsorption characteristics other than those of IGF 1I125 — a subject remaining open for future analyses.

Manufacturer Code	Tube Code	Sterile
Greiner Bio-One	G1 (300 µL Cryo.s™ Biobanking Tubes, non-sterile)	-
	G2 (300 µL Cryo.s™ Biobanking Tubes, sterile)	•
A	A1	-
B	B1	-
C	C1	-
D	D1	•
	D2	-

Table 2: 96-way cryogenic storage tubes from different suppliers were tested in the IGF 1I125 adsorption test. Greiner Bio-One all other tube manufacturers are anonymized and tube codes are utilized to differentiate between different tube types offered by individual manufacturers (e.g., manufacturer 'D' offers the two different tube types 'D1' and 'D2').

Description	Cat. No.	Case of
Cryo.s™ Sample Tubes with Datamatrix Coding		
Cryo.s Sample Tubes with Datamatrix, 1–1.2 mL	**89176-678**	**500**
Cryo.s Sample Tubes with Datamatrix, up to 2.2 mL	**89176-674**	**500**
Cryo.s Sample Tubes with Datamatrix, 1.8–2.0 mL	**89176-676**	**500**
Cryo.s™ Biobanking Tubes with Datamatrix Coding		
Racks with 96 Cryo.s Biobanking Tubes, Datamatrix Coded, 300 µL	**75832-302**	**960**
Racks with 96 Cryo.s Biobanking Tubes, Datamatrix Coded, 600 µL	**75832-304**	**960**
Racks with 96 Cryo.s Biobanking Tubes, Datamatrix Coded, 1000 µL	**75832-306**	**960**

VWR COLLECTION designed for precision

New EHP and UHP Pipettor Starter Kits

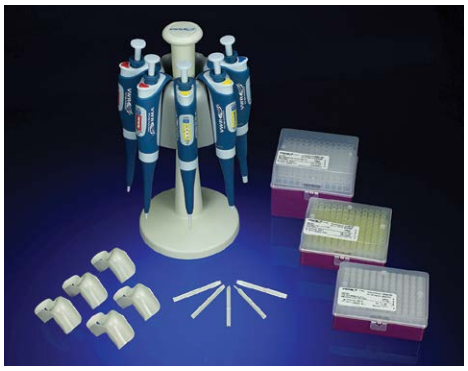

VWR Stands Available

- EHP Pipettor Starter Kits with four pipettor linear stand
- UHP Pipetttor Starter Kits with eight pipettor multiple stand
- New Five Pack UHP Pipettor Starter Kit covering 0.2-1000µL

New Starter Kits include various combinations of pipettors, pipettor stand, and pipette tips. EHP Starter Kits are available in three or four packs, while UHP Starter kits are available in three, four, or five packs. VWR stands are also available as accessories with space for one, four, six, or eight pipettors.

Description	Cat. No.	Unit
VWR EHP 3 Pack (incl. 10, 100, 1000µL pipettors & 4 pipette linear stand)	**75788-458**	**Each**
VWR EHP 3 Pack (incl. 20, 200, 1000µL pipettors & 4 pipette linear stand)	**75788-456**	**Each**
VWR EHP 4 Pack (incl. 10, 20, 200, 1000µL pipettors & 4 pipette linear stand)	**75788-460**	**Each**
VWR UHP 3 Pack (incl. 10, 100, 1000µL pipettors & 8 pipette multiple stand)	**75786-296**	**Each**
VWR UHP 3 Pack (incl. 20, 200, 1000µL pipettors & 8 pipette multiple stand)	**75788-462**	**Each**
VWR UHP 4 Pack (incl. 10, 20, 200, 1000µL pipettors & 8 pipette multiple stand)	**75786-304**	**Each**
VWR UHP 5 Pack (incl. 2, 10, 20, 200, 1000µL pipettors & 8 pipette multiple stand)	**75786-354**	**Each**
VWR 8 Pipettor Multiple Stand	**75788-466**	**Each**

Organoid Research Reagents

biogems A PeproTech Brand PEPROTECH OUR SUPPORT, YOUR DISCOVERY

Premium Quality Products to Support Your Research

- Used to efficiently generate, grow, and maintain organoids
- Guaranteed high purity and lot-to-lot consistency
- Bulk production and scale up capabilities available

US ONLY

Organoid models are three-dimensional (3D) cell culture systems that closely resemble in-vivo organs or tissues. These 3D systems reproduce the complex spatial morphology of a differentiated tissue to allow biologically relevant cell-cell and cell-matrix interactions. They are useful in a variety of applications including disease modeling, drug testing, toxicity screening, organogenesis modeling, and regenerative medicine. The accompanying table includes a selection of the common PeproTech Recombinant Proteins and BioGems Small Molecules used to generate, grow, and maintain these cell cultures.

Description	Size	Cat. No.	Unit
Recombinant Human R-Spondin-1	20 µg	**10779-202**	**Each**
Recombinant Human Noggin	20 µg	**10772-456**	**Each**
Recombinant Human EGF	500 µg	**10781-694**	**Each**
Human FGF-basic	50 µg	**10778-900**	**Each**
Forskolin	10 mg	**75844-686**	**Each**
Prostaglandin E2	50 mg	**75844-542**	**Each**
SB 202190	25 mg	**75844-886**	**Each**
Y-27632 Dihydrochloride	10 mg	**75844-614**	**Each**

These products are not available in Canada. Please contact your VWR Sales Rep to learn about easy access to similar options in your region.

Corning® Matrigel® Basement Membrane Matrix

CORNING

Certified LDEV-Free

Corning Human Umbilical Vein Endothelial Cells (HUVEC-2) stained with Calcein AM and cultured on Corning Matrigel matrix.

Corning Matrigel basement membrane matrix is a solubilized basement membrane preparation extracted from the Engelbreth-Holm-Swarm (EHS) mouse sarcoma, a tumor rich in extracellular matrix proteins to include laminin (a major component), collagen IV, heparan sulfate proteoglycans, and entactin/nidogen[1,2]. Corning Matrigel matrix also contains TGF-beta, epidermal growth factor, insulin-like growth factor, fibroblast growth factor, tissue plasminogen activator[3,4], and other growth factors which occur naturally in the EHS tumor.

Corning Matrigel basement membrane matrix is effective for the attachment and differentiation of both normal and transformed anchorage dependent epithelioid and other cell types. These include neurons[5,6], Sertoli cells[7], chick lens[8], vascular endothelial cells[9], and hepatocytes[10]. Corning Matrigel matrix will influence gene expression in adult rat hepatocytes[11] as well as three dimensional culture in mouse[12-15] and human[16,17] mammary epithelial cells. It will support *in vivo* peripheral nerve regeneration[18-20], can be used for metabolism and toxicology studies[21,22], and is the basis for several types of tumor cell invasion assays[23,24]. Corning Matrigel matrix provides the substrate necessary for the study of angiogenesis both *in vitro*[25,26] and *in vivo*[27-29]. Corning Matrigel matrix also supports *in vivo* propagation of human tumors in immunosuppressed mice[30-32].

Wide Selection of Basement Membrane Matrices

Corning Matrigel Matrix Growth Factor Reduced (GFR) is suited for applications where a more highly defined basement membrane preparation is desired. Available in standard Growth Factor Reduced (GFR), High Concentration (HC), and Phenol Red-free formats.

Corning Matrigel Matrix High Concentration is suited for in vivo applications where a high protein concentration augments growth of tumors. The high protein concentration also allows the Corning Matrigel matrix plug to maintain its integrity after subcutaneous injection into mice. Available in standard, GFR, and phenol red-free formats.

Corning Matrigel Matrix Phenol Red-free is recommended for assays which require color detection (i.e., fluorescence).

Corning Matrigel hESC-Qualified Matrix has been qualified as mTeSR®1-compatible by STEMCELL Technologies, thus eliminating the need for time-consuming screening in order to provide the reproducibility and consistency essential for your human embryonic stem (hES) cell research. The mTeSR1 formulation and Corning Matrigel matrix have been shown to be a successful combination for feeder-free maintenance of different WiCell™ hES cell lines for up to 20 passages (mTeSR1, STEMCELL Technologies).

Quality Control

- Mouse colonies are routinely screened for pathogens via Mouse Antibody Production (MAP) testing.
- Extensive PCR testing is performed to screen for a number of pathogens, including LDEV, to ensure strict control of raw materials used during the manufacturing process.
- Tested and found negative for bacteria, fungi, and mycoplasma.
- Protein concentrations are determined by Lowry method.
- Endotoxin units are measured by Limulus Amoebocyte Lysate assay.
- Corning Matrigel matrix gel stability is tested for a period of 14 days at 37°C.
- Biological activity is determined for each lot using a neurite outgrowth assay. Chick dorsal root ganglia are plated on a 1.0mm layer of Corning Matrigel matrix and must generate positive neurite outgrowth response after 48 hours without addition of nerve growth factor.

TYPICAL APPLICATIONS:

Cell Growth and Differentiation

Corning Matrigel matrix is especially suited for the culture of polarized cells, such as epithelial cells. It promotes the differentiation of many cells types including hepatocytes, neurons, mammary epithelial, endothelial, and smooth muscle cells.

In Vivo Angiogenesis Studies

Corning Matrigel matrix HC can be used to assess *in vivo* angiogenic activity of different compounds by subcutaneous injection into mice (Corning Matrigel plug assay). The plugs are subsequently removed and analyzed for the formation of blood vessels.

Augmentation of Tumor Growth in Nude Mice

Corning Matrigel matrix HC has been shown to promote successful transplantation of many human tumor cells including prostatic, breast, small-cell lung, colon, adrenal carcinomas, melanomas, and lymphoblastic leukemia cells. Also, it has been found to increase tumor growth rates *in vivo*.

Description	Size	Cat. No.	Qty/Cs
Corning Matrigel Matrix, LDEV-Free	10 mL	**47743-715**	**1**
Corning Matrigel Matrix, Phenol Red-Free, LDEV-Free	10 mL	**47743-716**	**1**
Corning Matrigel Matrix, (GFR), LDEV-Free	10 mL	**47743-720**	**1**
Corning Matrigel Matrix, (GFR), Phenol Red-Free, LDEV-Free	10 mL	**47743-722**	**1**
Corning Matrigel matrix, hESC qualified, LDEV-free	5 mL	**BD354277**	**1**

Development and Optimization of a High Titer Recombinant Lentivirus System

By Austin Storck, James Ludtke, Leisha Kopp, and Laura Juckem*

Introduction

Lentivirus is an enveloped single-stranded RNA virus from the Retroviridae family. Its ability to infect dividing and non-dividing cells has led to the widespread utilization of recombinant lentivirus as a gene delivery vehicle. In addition, lentivirus has an efficient integration mechanism which leads to robust and stable transgene expression in target cells.

Recombinant lentivirus production is accomplished in human embryonic kidney derived cells that stably express the SV40 large T antigen (e.g., 293T/17 cells). These cells are transiently transfected with three or four plasmids that encode the gene of interest (GOI) and the essential viral genes: gag, pol, and rev, along with the vesicular stomatitis virus envelope protein G (VSV-G). Once all the genes are expressed at sufficient levels, the virus is assembled and buds through the plasma membrane to form an enveloped virion pseudotyped with VSV-G that conveys the ability to transduce a broad range of mammalian cell types. The virus-containing supernatant can be collected and filtered to remove any cells.

Cell Confluency

A key parameter for successful transfection and subsequent virus production is the cell confluency at the time of transfection. Low confluency can lead to cytotoxicity and lower transfection efficiency. Performing transfections at high confluence (e.g., 85-90%) will maximize the protein expression levels and subsequent titers.

Reagent-to-DNA Ratio

The transfection reagent-to-DNA ratio is a critical parameter efficient nucleic acid delivery. The positively charged transfection reagent must be supplied in sufficient quantities in order to effectively condense and coat the negatively charged plasmid DNA. For ease of use, we formulated the *Trans*IT®-Lenti Transfection Reagent to work at a 3:1 reagent-to-DNA ratio (volume: weight). Altering the reagent-to-DNA ratio can adversely affect the virus titers (Figure 1). Similarly, we find a total plasmid concentration of 1µg/mL of culture to work best with the *Trans*IT®-Lenti Transfection Reagent.

The order of addition, composition, and stoichiometry of the plasmids can greatly influence the titers obtained. Depending on the virus generation, three or four plasmids need to be premixed

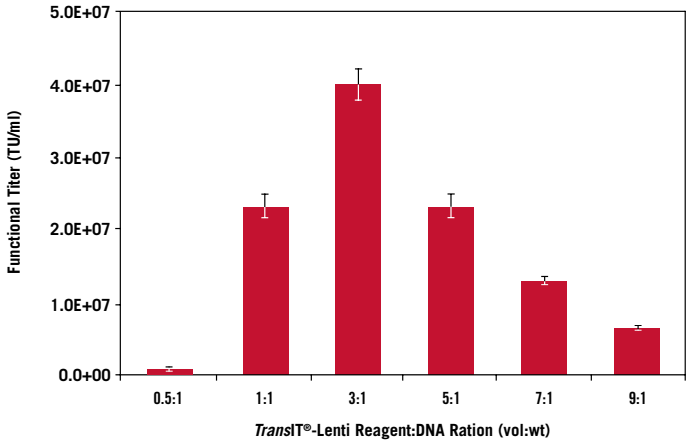

Figure 1. Optimization of Reagent-to-DNA Ratios. Adherent 293T/17 cells were transfected in a 12-well plate format using the pLKO.1-puro-CMV-TurboGFP™ transfer vector and the Lentivirus Packaging Mix, Powered by MISSION® Genomics (Mirus Bio) using the *Trans*IT®-Lenti Transfection Reagent (Mirus Bio) at varying reagent-to-DNA ratios (0.5:1-9:1). The supernatant was harvested, filtered (0.45µm), and titered using 293T/17 cells. Lentivirus transductions were performed in the presence of 8µg/ml *Transduce*IT™ (Mirus Bio) and GFP expression was measured 72 hours post-transduction using Guava® easyCyte™ 5HT Flow Cytometer (MilliporeSigma). Error bars represent the range of duplicate wells. Functional titers were calculated using virus dilutions with less than 20% GFP positive cells.

prior to being added to the complex to ensure that the transfection complexes are not formed preferentially with one plasmid over another. In addition, if using individual packaging plasmids, we recommend a starting ratio of 6:4:1:1 of transfer:gag-pol:rev:VSV-G vectors. If using a lentivirus packaging premixture, we recommend an initial ratio of 1:1 between the packaging mixture and the transfer plasmid.

Media Change Post-Transfection

The harvest procedure during recombinant lentivirus production often includes a media change 24 hours post-transfection, as well as multiple harvests at 48 and 72 hours post-transfection. To investigate the importance of these parameters, we tested the functional lentivirus titers in media samples post-transfection, as well as undisturbed at 48 and 72 hours post-transfection. By measuring the functional titers obtained from the media samples we found that the majority of the recombinant lentivirus was produced between 24–48 hours post-transfection (Figure 2). We also observed no difference in the functional lentivirus titers when

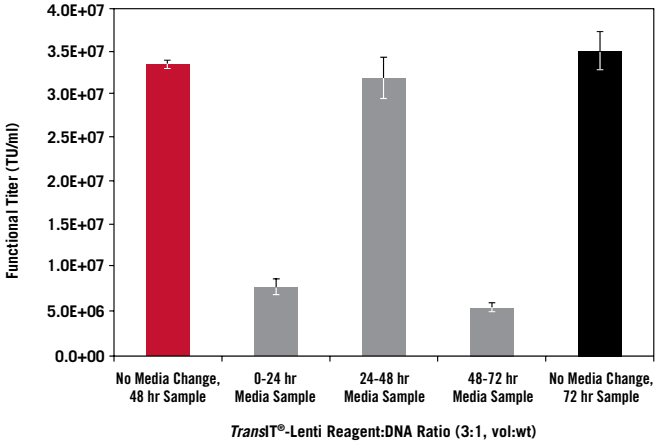

Figure 2. Single Harvest and No Media Change Required. Adherent 293T/17 cells were transfected in a 6-well plate with pLKO.1-puro-CMV-TurboGFP™ transfer vector and the Lentivirus Packaging Mix Powered by MISSION® Genomics (1:1 ratio, 2µg/well, Mirus Bio) with the *Trans*IT®-Lenti Transfection Reagent (Mirus Bio) at a 3:1 reagent-to-DNA ratio (vol:wt), The supernatant was harvested at the indicated time points, filtered (0.45µm), and titered using 293T/17 cells. Lentivirus transductions were performed in the presence of 8µg/ml *Transduce*IT™ (Mirus Bio) and GFP expression was measured 72 hours post-transduction using Guava® easyCyte™ 5HT Flow Cytometer (MilliporeSigma). Error bars represent the standard range of duplicate wells titered individually. Functional titers were calculated using virus dilutions with less than 20% GFP positive cells.

the virus is harvested at 48 or 72 hours post-transfection without a media change, suggesting that this step can be omitted without adverse affects. These findings demonstrate a workflow that reduces experimental complexity and workload.

Transfection Reagent Selection

High efficiency transfection is necessary, but not sufficient for high titer recombinant lentivirus production. To empirically determine the best transfection formulation for lentivirus production we initially screened our compound libraries using a reporter assay system; however, when we compared the reporter assay output with functional lentivirus production we did not always observe a correlation. Therefore, we employed a targeted compound screening approach to directly test the effect of reagent formulation on functional lentivirus titers. During this process we identified a novel formulation, the *Trans*IT®-Lenti Transfection Reagent, which yields up to 8-fold higher functional titers in head-to-head comparisons with other commonly used transfection technologies (Figure 3).
Vector design is a critical factor in recombinant lentivirus production. Advances in the safety of lentivirus production have been accomplished through the deletion of non-essential components of the virus genome, as well as separation of essential elements onto different plasmid vectors. In addition, the composition and design of the plasmid vector greatly affects the overall virus titer.

Transfer vectors encoding the GOI can be swapped while maintaining the same packaging vectors. In studying three different commercially available third generation transfer vectors we observed up to a 4-fold difference in lentivirus titers (Figure 4a). When performing system-to-system comparisons with different transfer vectors, packaging mixes, and transfection reagents the results are compounded to achieve a combined 100-fold difference between commercially available systems (Figure 4b). This illustrates the synergy between the essential components of recombinant lentivirus production.

Conclusions

We systematically optimized the experimental variables surrounding recombinant lentivirus production including: cell confluency, transfection reagent-to-DNA ratio, media change, incubation time, reagent formulation, and DNA vectors. The highest titers are achieved when 293T/17 cells are transfected at 90% confluency using the *Trans*IT®-Lenti Transfection Reagent at a 3:1 reagent-to-DNA ratio (vol:wt). A media change is not

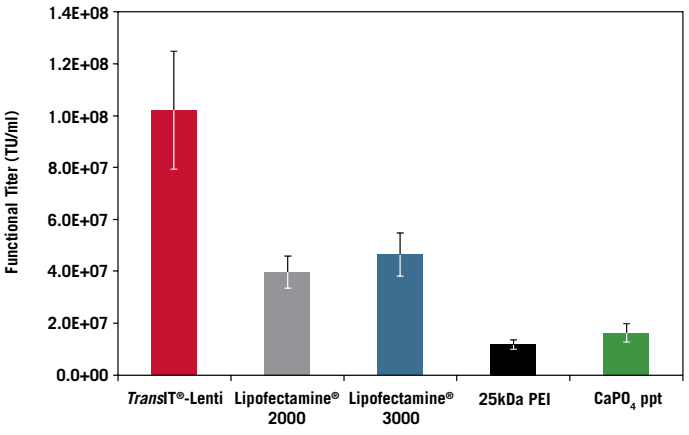

Figure 3. High Functional Titers with the TransIT®-Lenti Transfection Reagent. Adherent 293T/17 cells were transfected in a 6-well plate with pLKO.1-puro-CMV-TurboGFP™ transfer vector and the Lentivirus Packaging Mix Powered by MISSION® Genomics (1:1 ratio, 2µg/well, Mirus Bio) with the following reagents: *Trans*IT®-Lenti (3:1, vol:wt, Mirus Bio), Lipofectamine® 2000 (3:1, Thermo Scientific), Lipofectamine® 3000 (3:1:1, Thermo Scientific), 25kDa PEI (6:1, Polysciences), or $CaPO_4$ precipitation (4µg pDNA/well, GE Healthcare). The supernatant was harvested, filtered (0.45µm), and titered using 293T/17 cells. Lentivirus transductions were performed in the presence of 8µg/ml *Transduce*IT™ (Mirus Bio) and GFP expression was measured 72 hours post-transduction using Guava® easyCyte™ 5HT Flow Cytometer (MilliporeSigma). Error bars represent the standard deviation of triplicate transfection complexes titered individually. Functional titers were calculated using virus dilutions with less than 20% GFP positive cells.

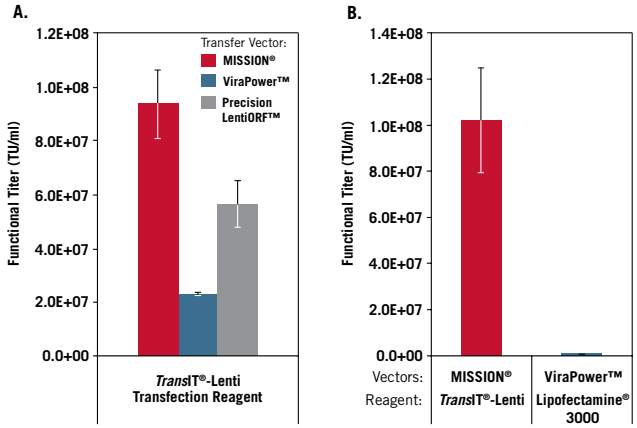

Figure 4. Vector Selection Greatly Affects Lentivirus Titer. (A) Adherent 293T/17 cells were transfected in a 6-well plate with one of three transfer vectors: MISSION® pLKO.1-puro-CMV-TurboGFP™ (MilliporeSigma), ViraPower™ pLenti6.2-GW/EmGFP (Thermo Scientific), or Precision Lenti-ORF™ RFP (GE Healthcare), and the Lentivirus Packaging Mix Powered by MISSION® Genomics (total 2µg/well, MirusBio) using the *Trans*IT®-Lenti Transfection Reagent (3:1, vol:wt, Mirus Bio). or **(B)** System-to-system comparisons were performed using either MISSION® pLKO.1-puro-CMV-TurboGFP™ transfection vector transfection vector and Lentiviral Packaging Mix (MilliporeSigma) and the *Trans*IT-Lenti Transfection Reagent or ViraPower™ (pLenti6.2-GW/EmGFP transfection vectors and Lentiviral Packaging Mix (Thermo Scientific) and the Lipofectamine® 3000 Transfection Reagent (Thermo Scientific) according to the manufacturers protocol. The supernatant was harvested, filtered (0.45µm), and titered using 293T/17 cells. Lentivirus transductions were performed in the presence of 8µg/ml *Transduce*IT™ (Mirus Bio) and GFP was measured 72 hours post-transduction using Guava® easyCyte™ 5HT Flow Cytometer (MilliporeSigma). Error bars represent the standard deviation of triplicate transfection complexes titered individually. Functional titers were calculated using virus dilutions with less than 20% GFP positive cells.

required post-transfection and a single harvest at 48 hours post-transfection offers convenience and less handling of the cells. In addition, the transfer and packaging plasmid also play a critical role in the titers achieved. The combination of transfection reagent, transfer vector and packaging premix can lead to a 100-fold difference in titers in head-to-head comparisons. The *Trans*IT®-Lenti Transfection System combining Mirus' novel transfection formulation and the MISSION® Lentivirus Packaging Plasmids provides exceptional lentivirus titers, increased flexibility, and reduced workload.

US ONLY

Description	Size, mL	Cat. No.
*Trans*IT-Lenti Transfection Reagent	1.5	75814-980
*Trans*T-Lenti Transfection Reagent	0.3	75814-982
*Trans*IT-Lenti Transfection Reagent	0.75	75814-984
*Trans*IT-Lenti Transfection Reagent	10 x 1.5 mL (15 mL)	75814-994
*Trans*IT-Lenti Transfection Reagent	5 x 1.5 mL (7.5 mL)	75814-986
*Transduce*IT Reagent	1	75814-996

These products are not available in Canada. Please contact your VWR Sales Rep to learn about easy access to similar options in your region.

NxSeq® AmpFREE Low DNA Library Kit

Generate Better NGS Data with PCR-Free, High-Efficiency Illumina DNA Libraries

Lucigen®

Next Gen Sequencing

- **Flexible:** Build libraries with only 75 ng up to 1 µg of sheared gDNA
- **High Efficiency:** Generate more sequenceable fragments and more data from each sample
- **PCR-free:** Prevent any introduction of PCR bias and uneven coverage

NxSeq AmpFREE Low DNA Library Kits contain Enzyme Mix, 2X Buffer, Ligase, and Elution Buffer. Adaptors must be purchased separately. Each NxSeq Adaptor box contains 12 different indexed Illumina-compatible adaptors with enough of each adapter for four library reactions. Box 1 contains adaptors 1-12 and Box 2 contains adapters 13-24.

Description	Cat. No.	Unit
NxSeq AmpFREE Low DNA Library Kit, 12 libraries	**10837-142**	**Each**
NxSeq AmpFREE Low DNA Library Kit, 48 libraries	**10837-144**	**Each**
NxSeq Adaptors, Box 1	**10837-146**	**Each**
NxSeq Adaptors, Box 2	**10837-148**	**Each**

VWR COLLECTION

designed for reliability

VWR® Ultra Low Temperature Upright Freezers

VWR Ultra Low Temperature (ULT) freezers are designed and constructed for long-term performance, and they represent the leading choice of laboratory professionals for applications where temperature control is critical.

- Temperature Range: –86 to –50°C (–123 to –58°F)
- Microprocessor temperature control system
- Advanced monitor/alarm system
- Automatic voltage compensator
- Cascade refrigeration system
- Non-CFC, non-HFCF, nonflammable refrigerants
- VWR two-year limited parts and labor warranty
- VWR five-year warranty on compressor parts

These freezers offers a microprocessor temperature control system that maintains constant freezer temperature, along with a sophisticated microprocessor monitor/alarm system. The microprocessor temperature control system can be set in 1° increments. The microprocessor monitor/alarm system features audible and visual indicators to keep the operator informed of over/under-temperature conditions, power failures, low battery, and door ajar scenarios. LED indicates actual chamber temperature. Air-cooled, hermetically-sealed dual compressors work in unison and cycle on demand of the microprocessor temperature controller. The automatic voltage compensator detects line frequency, monitors incoming voltage, and adjusts compressor voltage to reduce wear and tear on the compressors.

Volume, L (cu. ft.)	Electrical	Cat. No.	Unit
368 (13)	120V, 60Hz	**10160-724**	**Each**
368 (13)	208/230V, 60Hz	**10160-726**	**Each**
490 (17.3)	120V, 60Hz	**10160-728**	**Each**
490 (17.3)	208/230V, 60Hz	**10160-730**	**Each**
651 (23)	120V, 60Hz	**10160-732**	**Each**
651 (23)	208/230V, 60Hz	**10160-734**	**Each**
793 (28)	208/230V, 60Hz	**10160-736**	**Each**

PerfeCTa® SYBR® Green SuperMix/FastMix®

Sensitive and Precise DNA Amplification with SYBR-based Quantification

- 2x concentrated reagents minimize pipetting steps, simplify reaction assembly, and improve accuracy
- Superior assay sensitivity and specificity with ultrapure AccuStart™ enzyme technology
- Maximum-yielding Taq DNA polymerase mutant controlled by stringent, multi-epitope antibody hot start
- Supports efficient vortex mixing with proprietary anti-foaming formulation

PerfeCTa SYBR Green SuperMix and FastMix ensure specific primer extension products with ultrapure AccuStart hot start technology and proprietary formulation that reduces potential for primer-dimer and other non-specific artifacts. Single-tube reagents are 2X concentrated ready-to-use reaction cocktails containing all necessary components for quantitative PCR, except primers and DNA template. The proprietary formulation stabilizes the SYBR Green I dye to deliver maximum efficiency, sensitivity, and robust fluorescent signal.

Description	Cat. No.
PerfeCTa SYBR Green SuperMix	101414-150
PerfeCTa SYBR Green SuperMix for IQ	101414-142
PerfeCTa SYBR Green SuperMix with ROX	101414-158
PerfeCTa SYBR Green SuperMix with Low ROX	101414-166

Get More Colonies from Gibson Assembly® Transformations

E. cloni® 10G Chemically Competent Cells and Epicentre Transformax™ EPI300* Electrocompetent Cells*

- Endorsed by SGI-DNA for BioXp™ 3200 System and Gibson Assembly applications
- Increase colony counts with high efficiency competent cells
- Read the App Note! **vwr.com/gibson-e.cloni**

*Now available exclusively through Lucigen.

Size	Cat. No.	Unit
E. cloni® 10G Chemically Competent Cells (≥1 x 10^9 cfu/µg DNA)		
12 reactions, SOLOs	89005-078	Each
24 reactions, SOLOs	89005-080	Each
48 reactions, SOLOs	89005-082	Each
12 reactions, DUOs	89002-674	Each
24 reactions, DUOs	89002-676	Each
48 reactions, DUOs	89002-678	Each
96 reactions, DUOs	89002-680	Each
TransforMax™ EPI300™ Electrocompetent E. coli (≥1 x 10^{10} cfu/µg DNA)		
20 reactions, 10 x 100 µL	75927-928	Each
50 reactions, 50 x 100 µL	75927-930	Each

Pipetting Ergonomics

Pipettes, the workhorses of laboratories, are used for accurate transfer of microliter volumes of liquids from one vessel to another. Operating a pipette involves a considerable amount of muscle work. Firstly, the thumb muscles controlling the plunger movement and tip ejector are under a lot of strain. Secondly, as pipettes are typically held away from the body with the arm in an elevated position, the muscles in the arms, shoulders, and upper back are under static load. Thirdly, due to the precise nature of the work, the neck is often bent forward. Lastly, work in isolators or under laminar flow increases the risk of uncomfortable, non-neutral working positions.

Pipetting can be thought of as a cycle consisting of four distinct steps: adjustment of pipetting volume, tip attachment, aspiration, and dispensing; including repeated pressing and releasing of the operating button and detaching the used pipette tip. The required forces and activated muscles differ in different phases of the cycle. The thumb is under heavy load during aspiration, dispensing, and tip ejection, whereas the muscle load during volume adjustment and tip attachment spreads to a greater area of the hand, arm, and shoulder region.

Pipetting is repetitive work that may continue for long periods of time, even throughout entire working days. Due to its repetitive nature and the related load on musculoskeletal structures, the ergonomic aspects of pipetting have been the focus of researchers for several decades. Laboratory work involving pipetting was first associated with an increased risk of upper body musculoskeletal disorders in the 1990s[1-3]. Since then, several articles have been published that address various aspects of pipetting ergonomics.

This article reviews the published literature on pipetting ergonomics and covers the following topics:

- Factors influencing the development of pipetting related musculoskeletal disorders
- Solutions for lowering the risk for musculoskeletal disorders.

FACTORS INFLUENCING THE DEVELOPMENT OF PIPETTING RELATED MUSCULOSKELETAL DISORDERS

Since Fredriksson and Bjorksten et al. discovered the connection between pipetting hours and musculoskeletal disorders in the 1990s, a significant number of studies relating to pipetting ergonomics have been published. Many studies have focused on the influencing factors behind the development of musculoskeletal disorders and emphasize analyzing anthropomorphic data. Research has also been conducted on working environments, such as the effect of working positions and workbench height on pipetting ergonomics.

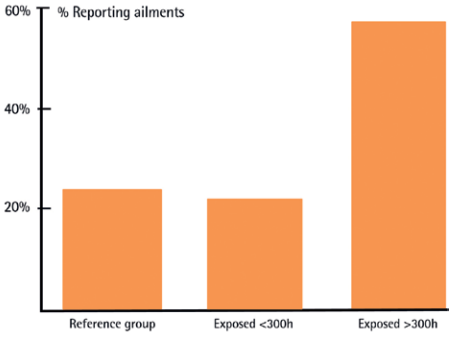

Figure 1. Reported hand and shoulder ailments of groups exposed to different amounts of pipetting. Image re-drawn from[1].

The force distribution within the pipetting cycle is also well understood. Understanding the reasons behind how pipetting related musculoskeletal disorders develop provides tools not only for designing pipettes with improved ergonomics but also for designing laboratory environments and workflows to support the wellbeing of laboratory professionals.

The Influence of Pipetting Hours

The Bjorkesten et al. study indicates that more than 300 hours a year of pipetting leads to an elevated risk of hand and shoulder ailments (Figure 1)[1]. David and Buckle set the hourly limit lower, and state that the percentage of people reporting hand problems increases for those pipetting more than 220 hours a year[3]. David and Buckle discovered that hand complaints were significantly more frequent with individuals whose job included continuous pipetting for more than 30 minutes, compared to those only pipetting continuously for shorter periods of time (Figure 2). Increasing pipetting for more than 30 continuous minutes further

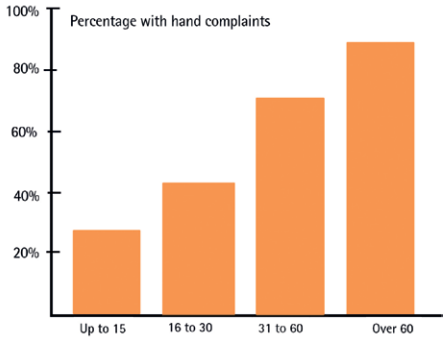

Figure 2. Number of minutes continuously pipetting and the corresponding percentage of workers with hand complaints. Image re-drawn from[3].

increased the amount of hand complaints: 90% of users pipetting for more than 60 continuous minutes reported problems[3].

When comparing the tendon displacement data with earlier findings from typing measurements, it was concluded that it would require three hours of continuous pipetting daily to reach a medium risk level for musculoskeletal disorders. Even for the test subject with the highest tendon displacement data it would require two hours of continuous daily pipetting to reach the medium risk level for musculoskeletal disorders[16, 21]. Wu admits that based on earlier findings, the tendon displacement data seems to underestimate the risk for musculoskeletal disorders. The differing results could be explained by the fact that although tendon displacement data might be comparable with, for example, typing, the forces in pipetting are much higher, which is an important contributing factor[16].

Despite all the evidence about the connection between pipetting and musculoskeletal disorders, there are no generally accepted and applied recommendations or guidelines for safe daily exposure to manual pipetting.

The Effect of Gender and Age

Generally, women are more prone to pipetting related musculoskeletal problems than men. This is due to the fact that women typically have weaker muscles that get tired more easily. Fredriksson discovered that for women with the weakest muscular structures, the force needed to operate a mechanical pipette was unacceptably high, corresponding to 29% of their maximum capacity. For men the force was 15% of their maximum capacity, which was considered an acceptable level of stress[2]. It is important to note that the other potential risk factors related to pipetting ergonomics, such as awkward positions and static muscle load in the upper part of the body, don't differ between men and women.

Pipetting related stress symptoms typically increase with age and time spent pipetting[2]. A survey conducted by David et al confirmed the connection between age and percentage of complaints, with complaints increasing in both the pipette user and the control group after the age of 35[3].

Awkward Positions

Although pipetting related ergonomic problems are most often connected with the heaviness of plunger operation and the stress related to thumb movement, David and Buckle discovered that a higher percentage of pipette users that reported hand or neck problems had adopted awkward or fixed postures when using pipettes compared to those who didn't have any problems[3].

Muscle activity in the shoulder and upper back region can be reduced by using arm supports. Gel pad type supports help to reduce contact stress for the elbow. However, there is a risk of adopting a compromised wrist posture, especially when using gel pad type supports. When placing an elbow on the pad, the wrist may need to be flexed to reach tubes that are closer to the elbow. To ensure an ergonomic working posture, attention should be paid to the position of the wrist when using a gel pad support[10].

High and Low-Precision Tasks

Asundi et al. discovered that there is a clear difference in static muscle activity between high and low-precision pipetting tasks. High-precision tasks, such as pipetting a liquid from on top of another liquid or gel and avoiding transferring any of the lower medium, significantly increased static muscle activity. High-precision pipetting requires greater control of thumb motion, which increases static muscle load. High precision tasks were also found to reduce peak thumb force by 5% compared to low precision tasks, most likely due to greater control while pressing the plunger[8].

Pipetting Speed

The results obtained by Srinivasan et al. indicate that when pipetting pace increases, both the amount and structure of motor variability in the shoulder and elbow decrease. These results suggest that motor variability drops when repetitive movements are carried out at an increased pace, which may in the long run lead to muscle fatigue or overuse. It's important to note, however, that the interpretation of motor variability changes in the context of occupational health, well-being, and performance is not fully developed and further research is still required[14].

Liquid Viscosity

Pipetting high-viscosity fluid increases peak thumb force by 11% compared to low-viscosity fluids. This is most likely due to greater resistance during dispensing[8].

Force Distribution within the Pipetting Cycle

Asundi et al. examined the force used during the pipetting cycle and learned that it is at its highest during the liquid dispense and blow-out phase (Figure 3)[8]. Wu et al. quantified the peak push force during

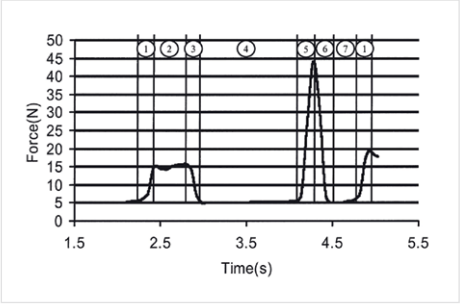

Figure 3. Typical force profile during pipetting. Explanations of the different pipetting phases: (1) pressing the plunger, (2) holding the plunger down, (3) releasing the plunger to aspirate, (4) locating the target vessel –no force applied, (5) pressing the plunger for dispensing and blow-out, (6) releasing the plunger, (7) locating the next sample. Image re-drawn from[8].

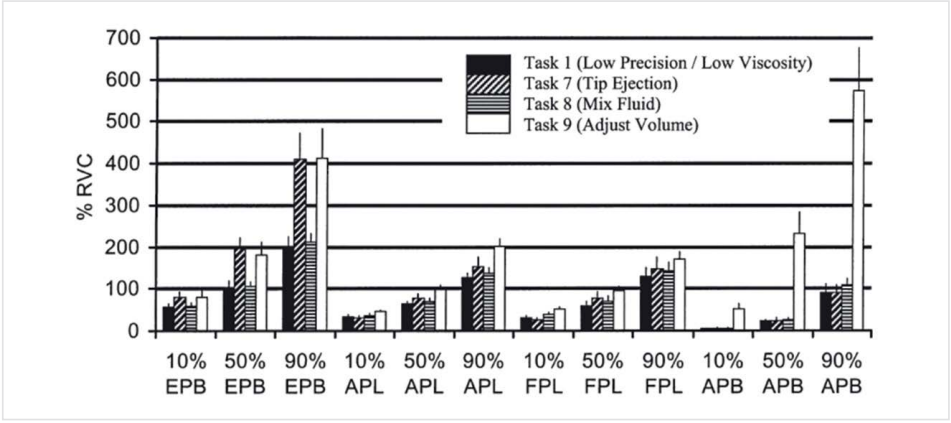

Figure 4. Reference voluntary contraction (RVC) of the four muscles studied (extensor pollicis brevis (EPB), abductor pollicis longus (APL), flexor pollicis longus (FPL), and abductor pollicis brevis (APB)) describes the force required in four different pipetting tasks at 10% (static activity), 50% (median activity), and 90% (peak activity). Task 1: Transfer 100µL of water from a 50mL centrifuge tube into a 15mL centrifuge tube. Task 7: Attach a tip from a tip rack box onto a pipette, then eject the tip and repeat five times. Task 8: Transfer 100µL of water from a 1.5mL microcentrifuge tube to a similar tube. Mix five times. Task 9: Adjust a pipette from 200µL to 20µL to 200µL by turning the volume adjustment dial. Image re-drawn from[8].

dispensing to be typically 2.5–3.0 times the force required for aspiration, and the mean peak force to be 3.2 times the force used for aspiration[17].

Asundi discovered that of all pipetting related tasks, volume adjustment produced the highest level of muscle activity. This task involves turning the volume adjustment dial with the thumb and index finger. The small diameter of the dial, the limited contact friction between the dial and the fingers, and the force required to turn the dial may explain the high levels of muscle activity during this task. Tip ejection also requires a high level of muscle activity (Figure 4)[8].

SOLUTIONS FOR PREVENTING THE RISK OF MUSCULOSKELETAL DISORDERS

There are significant differences between the ergonomic design of hand-held pipettes. However, in addition to selecting ergonomic tools, it is important to pay attention to personal working habits. This section summarizes the published research about the ways of preventing musculoskeletal disorders originating from pipetting.

An Ergonomic Design for Mechanical Pipettes

Research connecting pipette design with musculoskeletal disorders has mainly concerned single-channel mechanical pipettes. Despite all the published articles on the topic, there are no published studies available where the influence of pipette properties has been examined systematically and where the effect of individual parameters could be ascertained. Although claims have been made for the effect of pipette height, weight, and other factors on ergonomics, they are all multivariate systems, and, more often than not, the effect of individual parameters can't be fully understood.

The book *Ergonomic Checkpoints* lists the following points to consider when designing any hand tools. As even slight muscle fatigue reduces output in tasks where precise movements are important, to maintain performance, tools which requir high forces should be avoided. Similarly, heavy tools will tire the user, whereas tools with minimal weight allow precise operations. Hand tools need a grip with proper dimensions and properties: a handle diameter of 30–40mm and a handle length of at least 100mm, with a length of 125mm being more comfortable. Adequate friction is also required to prevent slipping and to reduce the need to squeeze. A noncircular cross-section reduces rotation in the hand[22].

One idea to improve pipette ergonomics is to tailor the dimensions and features according to user dimensions or other properties. When examining the correlation between different pipette designs and user experience, Lichty et al. found no connection between user anthropology (e.g., hand size, grip strength, or other individual user characteristics) and the pipette usability ratings or hand and arm comfort. This indicates that pipettes can't be recommended to users based on their hand sizes. The same study, however, found a correlation between hand, arm, and grip comfort and the following pipette subjective measures: pipette balance, accuracy, plunger comfort, and tip ejector usability. User comfort was found to correlate negatively with the two pipette

physical properties of blowout and tip ejection force. Better pipette balance correlated with lower pipette weight. Of the pipette features, the volume adjustment usability rating was found to have a strong correlation with experienced productivity. Smaller pipette handle girth and lower weight were associated with measured productivity (shorter time to perform tasks). It is important to note that study participants admitted to favoring familiar designs with familiar controls that can be accessed quickly when needed[18].

The higher muscular load on the hand exerts a higher risk for upper extremity disorders, especially carpal tunnel syndrome (CTS)[11]. The ergonomics and usability characteristics of six mechanical pipettes were evaluated and the collected data combined with biomechanical load recordings (muscular activity and wrist postures) and user-reported usability evaluations. The collected electromyography (EMG) data indicated that the heaviest and longest pipette with a short finger rest created the highest muscular activity, whereas the shortest and lightest pipette caused less muscular activity. The shortest and lightest pipette also helped to maintain the most neutral wrist position during pipetting compared to the longest and heaviest pipettes[11]. The Sormunen et al study found a correlation between overall pipette usability and pipette weight and length: user assessments of comfort, usability, and functionality were the highest for the three lightest and shortest pipettes with more curved finger rests. Users experienced increased neck, shoulder, wrist, hand, and finger strain when using the heaviest and longest pipette. To summarize, users rated the lighter and shorter pipettes as more usable and comfortable. The comfort experienced was supported by the lower biomechanical load measured during pipetting[17].

When comparing muscular activity during the use of five different mechanical pipettes it was observed that the load was similar in three of the four muscles examined (flexor pollicis brevis — flexing the thumb at the metacarpophalangeal joint, flexion, and medial rotation of the first metacarpal bone at the carpometacarpal joint; flexor digitorum sublimis — flexion of the middle phalanges at the proximal interphalangeal joint; and trapezius — the support to arm weight, retraction, medial rotation, and repression of scapula). Only the activity of flexor pollicis longus differed between the pipettes, and this was the lowest with the shortest and lightest pipette. The low activity was considered to be due to the lightness of the plunger button and the low degree of ulnar deviation in the wrist, which was significantly lower for this pipette. The related user perception study was aligned with the muscular activity measurements as the perceived strain was the smallest for the shortest and lightest pipette. Despite the differing results in muscular activity, the use of all the pipettes resulted in non-neutral wrist posture (angles from 20–27 degrees), with the extension being the greatest with the longest pipette[9].

Asundi et al. discovered that of all pipetting related tasks volume adjustment produced the highest level of muscle activity. Based on these results, they suggested the following modifications to pipette design: increased diameter of the volume adjustment dial and reduction of the required rotation force[8].

To summarize the findings on pipette properties, the research literature connects the following pipette features with improved ergonomics and usability: short length, light weight, pipette balance, plunger comfort, and tip ejector usability. Blow-out force and high tip ejection force have a negative correlation with experienced ergonomics. Smaller pipette handle girth, lower weight, and volume adjustment correlate positively with experienced productivity[9, 11, 18].

The Ergonomics of Electronic Pipettes

Electronic pipettes were developed to make pipetting less work for the user and thus avoid the development of musculoskeletal disorders caused by muscle overuse. The muscle work performed by the user is taken over by the machinery of the electronic pipette, making it possible even for workers already affected by musculoskeletal disorder (MSD) to continue performing pipetting tasks. Despite their long presence in the market, the ergonomics of electronic pipettes has been studied surprisingly little.

One study examined the influence of electronic multichannel pipettes on muscle load in the shoulder and right arm during pipetting tasks using three commercially available electronic pipettes. The main conclusion was that the tested pipettes differed less in ergonomics and usability than previously examined mechanical single-channel pipettes. No differences were observed in the user benefits of the different pipette designs, their fit and balance in the hand, or finger hook design. Moreover, no differences were found in the muscle activity in the shoulder and right arm or in the wrist joint angle. Differences were, however, observed in the thumb static muscle load, with one of the pipettes causing heavier load than the other two. This might be explained by the unique aspiration and dispensing mechanism operated by the index finger instead of the thumb, which keeps the thumb muscles activated. Interestingly, despite the higher muscle load measured, users experienced this pipette as less straining on the thumb than the other pipettes tested. Users observed differences in the location and lightness of the tip ejector button. They also

pointed out the difficulties in finding a good grip for tip ejection and using the operating button in one pipette and poor tip attachment in another model. The appeal of the highest rated pipette was in its lightness, fit in the hand, the lightness of the tip ejection, and in pipette operation with the index finger[23].

Postures and Work Surface Height

Pipetting is performed at multiple workstations in laboratories, including standard workbenches and in laminar flow cabinets and isolators. Traditionally, workbenches have not been height adjustable. In such working environments it may be challenging for the tallest and shortest workers to find an optimal working posture. Today's modern laboratories have adjustable workbenches – even the height of laminar flow cabinets can be optimized for individual users.

There are no recommendations for the best workbench height for pipetting work. Generally, it is instructed that the hand should be at elbow height with the arm close to the chest to reduce stress on the shoulder region. However, the hand is quite often located well above the elbow during pipetting, which may result in wrist deviation and/or shoulder abduction.

When working in a seated posture, it is important to adjust the chair height to maintain the body in a neutral posture. When the workbench height can't be adjusted, a solid foot stool is required to support a neutral position. A chair foot ring is not recommended as it keeps knees in a bent position that risks blood vessels being squeezed or bruised[2].

Park et al. studied the influence of working surface height on muscle activity, posture, and discomfort while performing pipetting work in neutral standing and seated positions. The main conclusion was that in order to reduce shoulder strain without raising thumb and neck strain beyond acceptable limits, the laboratory workbench height should be at the level of the pipette tip when held in a standing position with hand at elbow height. The study recommended that pipetting work should not be done in a seated posture. When seated, muscle activity averaged 39% of isometric maximum voluntary contraction (MVC) for the anterior deltoid muscle that flexes and medially rotates the shoulder joint. This exceeds the recommended limit of maximum muscle activity, which is around 25–30% of MVC[5].

Workbench height significantly influences muscle activity, user-experienced discomfort, and wrist and neck posture. When the workbench height is increased, biomechanical stress and discomfort in the shoulder region also increase. At the same time the stress on the thumb and neck is reduced. This means that the risk of injuries and musculoskeletal disorders in the shoulder region increases with elevated workbench height. Lowering workbench height causes thumb muscle activity to increase. The effect, however, is not as dramatic as for the shoulder region. Activity levels remain around 20% MVC and below[5].

Workbench height also has an impact on the neck flexion angle, which highly increases when the workbench level is lowered. This indicates a higher risk for musculoskeletal disorders in the neck region when the workbench level is too low. Experienced discomfort forms a U-shaped curve with higher discomfort at both the lowest and highest workbench levels. The optimal workbench height is in the middle. The typical workbench height in laboratories (91–94cm) is too low for taller men (above 50th percentile) and too high for shorter women (below 50th percentile)[5].

In addition to the effects on the shoulder and neck region, workbench height also influences wrist posture in the radial/ulnar plane. However, the changes in wrist angle as a function of workbench height are small[5].

Arm Supports

Feng et al. compared the influence on muscle activity of different types of arm supports used during pipetting. The use of arm support significantly reduced muscle activity. Fixed and horizontal movable supports gave better results than springloaded support or no support at all[6]. Another study focused on evaluating the effect of two alternative arm supports on shoulder and upper back muscle loading during pipetting. The results indicated that both a gel pad and a freely moving counter-balanced forearm support resulted in significantly lower mean muscle activity. Mean muscle activity was the lowest with the gel pad support, and the highest without a support. Peak muscle activity in the anterior deltoid muscle was significantly reduced with the freely moving arm support. In addition to reduced muscle activity, higher comfort ratings were obtained when using arm supports. The users rated the gel pad as the best one for shoulder and upper back support. Having no support was rated the least comfortable by users[10].

These results suggest that arm support may be beneficial in reducing muscle loading and improving comfort for the shoulder and upper back during pipetting.

CONCLUSIONS

The connection between pipetting and musculoskeletal disorders is a well known fact. Since the first published articles in the early 1990s, pipetting ergonomics has been extensively studied from various angles. At the same time, laboratory

sartorius

personnel's awareness of pipetting ergonomics has greatly increased.

Pipetting not only strains the fingers and hand, it also strains the wrist, forearm, and shoulder — and even the neck and back. A high number of pipetting hours greatly increases the risk of developing pipetting related ergonomic problems. One to two hours a day of continuous pipetting already increases the risk of work-related neck and upper limb disorders (WRULDs). Women typically develop musculoskeletal problems more often than men due to weaker musculoskeletal structures. Stress symptoms also increase with age and time spent pipetting.

Ergonomic pipetting is a combination of multiple factors. Good pipette ergonomics is naturally very important. Pipetting ergonomics can be further improved with a proper hand support. Attention should be paid to having a good neutral working position (neck, lower back, hip, and knee) independent of working position (either standing or seated). Good ergonomics includes a working environment that is clean and safe to work in. All instruments and chemicals must be handled with proper competence and caution, lighting should be optimized for the task at hand, and the noise level must not be too high. Good working habits, such as breaks between long pipetting tasks, working close to the body, and using ergonomic working movements are also important for preventing ergonomics related problems.

Since the first studies in the 1990s, mechanical pipettes have become much lighter to operate. However, there are still big differences between the ergonomics of different pipette designs. Pipette purchasing decisions should therefore always involve evaluating the ergonomics, and pipettes should always be tested by users before making the final purchase decision. The entire pipetting cycle including volume adjustment, tip loading, aspiration and dispensing, and tip ejection should be evaluated. The fit in hand is an integral part of the ergonomics and thus the feel in hand should be optimal for the individual user. The pipette should be free from protruding parts and sharp edges that lower user comfort in the long run. When holding an ergonomic pipette in hand, it should feel light and well balanced — almost effortless.

Volume, µL	Cat. No.	Unit
Picus Single-Channel Pipettes		
0.2–10	**89233-092**	**Each**
5–120	**89233-094**	**Each**
10–300	**89233-096**	**Each**
50–1000	**89233-098**	**Each**
100–5000	**89233-100**	**Each**
500–10000	**89233-102**	**Each**
Picus 8-Channel Pipettes		
0.2–10	**89233-104**	**Each**
5–120	**89233-106**	**Each**
10–300	**89233-108**	**Each**
50–1200	**89233-110**	**Each**
Picus 12-Channel Pipettes		
0.2–10	**89233-112**	**Each**
5–120	**89233-114**	**Each**
10–300	**89233-116**	**Each**
50–1200	**89233-118**	**Each**

Produce *in vitro* Transcribed RNA FAST with the AmpliScribe™ T7-FLASH Transcription Kit!

Lucigen®

- Maximal RNA yields in only 30 minutes
- Highest yields available, ≥180 µg per reaction
- Makes long (≤9 kb) or short RNAs (≥25 bases) for CRISPR gRNA synthesis, *in vitro* translation, RNAi, and more

The AmpliScribe T7-FLASH Transcription Kits include AmpliScribe T7-Flash Enzyme Solution, AmpliScribe T7-Flash 10X Reaction Buffer, RNase-Free Water, RNase-Free DNase I, DTT, Control DNA Template (linearized), and RiboGuard™ RNase Inhibitor, as well as ATP, CTP, GTP, and UTP Solutions. Just add your DNA template containing a T7 RNA polymerase promoter and go!

Description	Rxn Size	Cat. No.	Unit
AmpliScribe T7-FLASH Transcription Kit	25	**75927-892**	**Each**
AmpliScribe T7-FLASH Transcription Kit	50	**75928-112**	**Each**

UVP GelStudio PLUS *touch*

analytikjena
An Endress+Hauser Company

Gel Documentation for Genomic and Proteomic Applications

- High resolution images with a 5 MP camera and a zoom f/1.2 lens, for close-up image capture
- A large 15.6", integrated touch screen computer; also available as a PC-controlled system for laboratories with specific IT requirements
- Automated software for image capture and enhancement settings
- Ergonomic, stand-alone design
- Thin-line transilluminator in a slide-out tray, automated filter wheel, and integrated UV Protection Shield for preparative work on gels

The UVP GelStudio PLUS imaging systems are essential to laboratories performing genomic and proteomic applications. The systems are customized for high resolution and sensitive imaging, of DNA gels, protein gels, blue/white excitable dyes, plants, colony plates, TLC plates, fluorescent dye applications, and more.

Description	Cat. No.	Unit
UVP GelStudio *touch*, 115 V	**75873-980**	**Each**
UVP GelStudio *touch*, 230V	**75873-978**	**Each**
UVP GelStudio, 115 V	**75873-984**	**Each**
UVP GelStudio, 230 V	**75873-982**	**Each**

VWR COLLECTION — designed for reliability

Lyse the Toughest Samples in Seconds

Rapid and Reproducible Extraction of Nucleic Acids, Proteins, and Small Molecules From Any Sample Type

- Simultaneously homogenizes 12x0.5mL, 4x1.5mL, 12x2mL, or 4x7mL samples
- Features a convenient front loading design with snap-in tube carriage
- 99 programmable memory settings and multilingual user interface

The VWR Bead Mill is part of the newest generation of bead mill homogenizers. This economical system is specifically designed for grinding, lysing, and homogenization of up to 16 samples. Using sample tubes pre-filled with a variety of lysing beads, the VWR Bead Mill vigorously and uniformly shakes the tubes, providing an efficient, consistent, high-yield, and quality homogenization usually in less than 40 seconds.

Description	Cat. No.	Unit
VWR Bead Mill Homogenizer	**75840-022**	**Each**
VWR 4-Place Mini Bead Mill	**10158-558**	**Each**
VWR Soft Tissue Homogenizing Mix, 0.5mL, 1.4mm Ceramic Beads	**10158-608**	**50 tubes**
VWR Soft Tissue Homogenizing Mix, 2mL, 1.4mm Ceramic Beads	**10158-610**	**50 tubes**
VWR Hard Tissue Grinding Mix, 2mL, 2.4mm Metal Beads	**10158-604**	**50 tubes**
VWR Hard Tissue Homogenizing Mix, 2mL, 2.8mm Ceramic Beads	**10158-612**	**50 tubes**
VWR Tough Microorganism Lysing Mix, 2mL, 0.05mm Glass Beads	**10158-606**	**50 tubes**

When Representative Genomic DNA Matters…

Distributor
GE Healthcare

Illustra™ Genomiphi DNA Amplification:

- Creates representative genomic DNA through isothermal amplification
- Outperforms PCR-based WGA techniques
- Leverages a quick and simple, automation friendly protocol (no thermocyclers required)

The GenomiPhi™ product range uses the Phi29 DNA polymerase to amplify large concentrations of DNA from small starting amounts of genomic DNA by isothermal multiple strand displacement amplification (MDA).

Description	Rxn Size	Cat. No.
illustra Single Cell GenomiPhi DNA Amplification Kit	25	10146-196
illustra Single Cell GenomiPhi DNA Amplification Kit	100	10146-198
illustra GenomiPh HYi DNA Amplification Kit	25	95042-268
illustra GenomiPh HYi DNA Amplification Kit	100	95040-348
illustra GenomiPhi V2 DNA Amplification Kits	25	95042-266
illustra GenomiPhi V2 DNA Amplification Kits	100	95040-352

Mag-Bind® TotalPure NGS

OMEGA bio-tek

Purification of DNA or RNA from Enzymatic Reactions in Next Generation Sequencing Workflows

- Consistent and reliable for both DNA and RNA clean-up
- Double-sided size selection capability
- Manual and automation-friendly sample processing in 96- and 384-well formats

Mag-Bind TotalPure NGS offers an easy-to-use, reliable solution for the purification of both DNA and RNA for next-generation sequencing workflows with high recovery rates. This product is designed for both manual and fully automated purification of DNA and RNA samples from a variety of enzymatic reactions including PCR, adaptor ligation, and cDNA synthesis. Purified DNA and RNA is suitable for a variety of downstream applications such as NGS library preparation, microarrays, automated fluorescent sequencing, and restriction enzyme digestion.

Description	Size, mL	Cat. No.	Unit
Mag-Bind TotalPure NGS	5	75877-714	Each
Mag-Bind TotalPure NGS	50	75877-716	Each
Mag-Bind TotalPure NGS	500	75877-718	Each

Development of a High-Throughput Data Analysis Method for Quantitative Real-Time PCR (qPCR)

By Gregory C. Patton, Ph.D., Andrew N. Gray, Ph.D., Nathan A. Tanner, Ph.D., Janine G. Borgaro, Ph.D., Yan Xu, Ph.D., Julie F. Menin, M.S. & Nicole M. Nichols, Ph.D., New England Biolabs, Inc.

Over the last 20 years, quantitative real-time PCR (qPCR) has become an essential technique in molecular biology for detecting and quantifying nucleic acids. Workflow simplicity and advances in instrumentation now permit sizable quantities of data to be generated rapidly, with 96, 384, or even 1536 reactions in one qPCR experiment. The challenge lies in the details: qPCR experiments require thoughtful design and analysis to capture all relevant information, such that accurate and appropriate conclusions can be drawn.

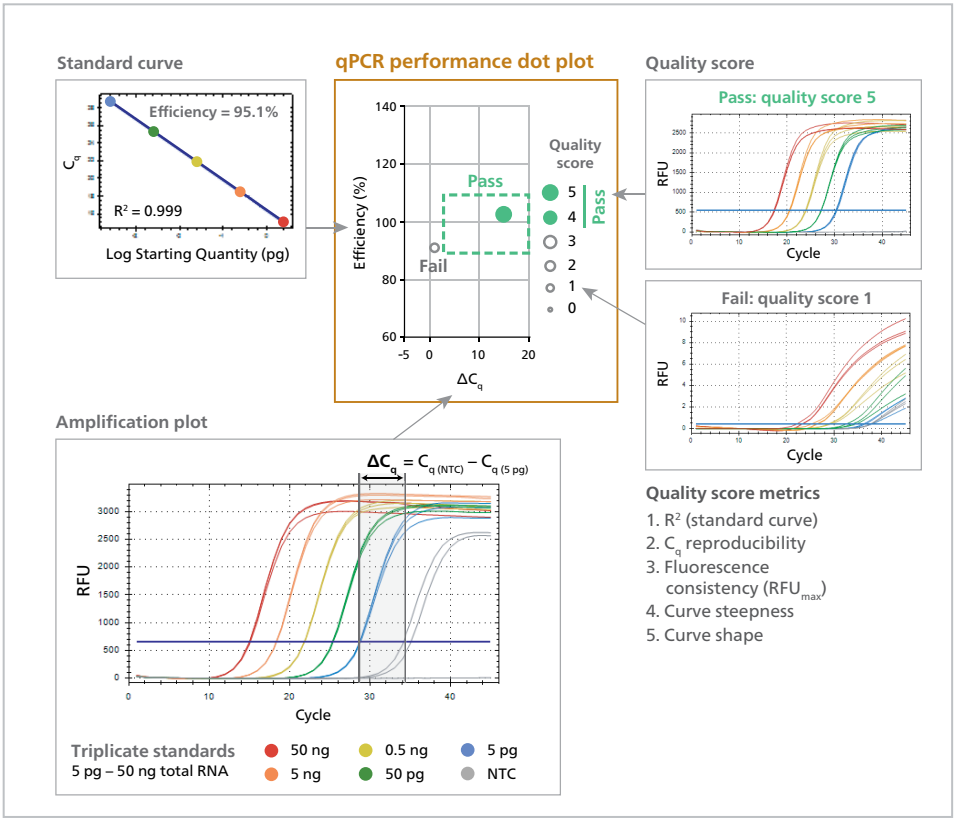

Figure 1. Breaking it down: how we translate qPCR data into dots in boxes.
NEB has developed a method to better evaluate the large amount of qPCR data generated in an experiment. The output of this analysis is known as a dot plot, and captures the key features of a successful, high-quality qPCR experiment as a single point. This method of analysis allows many targets and conditions to be compared in a single graph. For each experiment, triplicate reactions are set up across a five-log range of input template concentrations (Amplification plot, bottom-left). Three non-template control (NTC) reactions are also included, for a total of 18 reactions per condition/target. Efficiency (%) is calculated (Standard curve, top-left) and is plotted against ΔCq (dot plot, center), which is the difference between the average Cq of the NTC and lowest template dilution. This parameter captures both detection of the lowest input and non-template amplification. Acceptable performance criteria are defined as an Efficiency of 90-110% and a ΔCq of ≥ 3 (green box). Other performance criteria are captured using a 5-point Quality Score (top-right). The Quality Score is represented by the size and fill of the plotted dot, with experiments that pass all performance criteria represented by a solid dot within the box.

Development of NEB's Luna® qPCR product line required repeated data collection on a series of test panels, each containing multiple targets. In order to compare various amplicon panels over multiple qPCR runs, instruments, reagents, and conditions, a high-throughput data analysis method termed "dots in boxes" was developed. The output of this analysis captures key assay characteristics, highlighted in MIQE guidelines, as a single data point for each qPCR target. This method of analysis permits multiple targets and conditions to be compared in one graph, allowing concise visualization and rapid evaluation of overall experimental success.

Rapid adoption of qPCR and its relatively straightforward execution (mixing amplification reagents, primers, and template) has led to the generation of an enormous amount of data, as evidenced by the numerous publications containing qPCR experiments. However, the ease of generating qPCR data has also proven to be the technique's greatest challenge[1]. A diverse set of protocols, instruments, reagents, and analysis methods can be found in the scientific literature, with many publications reporting invalid or conflicting data. The lack of consensus on best experimental practices for qPCR resulted in the establishment of the Minimum Information for

NEW ENGLAND BioLabs Inc.

Publication of Quantitative Real-Time PCR Experiments (MIQE) guidelines by Bustin et al.[2]. The MIQE guidelines established a set of qPCR performance metrics that should be determined and reported in peer-reviewed publications to ensure robust assay performance and reproducibility. These assay characteristics include:

- PCR efficiency
- Dynamic range
- Limit of detection (LOD)
- Target specificity
- Precision

The fundamental performance criteria outlined in the MIQE publication therefore served as a basis for the development of a high-throughput data analysis method termed "dots in boxes" (Figure 1). For each amplicon, PCR efficiency, dynamic range, target specificity, and precision was captured as a single data point plotted in two dimensions, with the PCR efficiency plotted on the y-axis and the delta Cq (ΔCq) as the x-axis. ΔCq is the difference between the Cq values of the NTC and the lowest template dilution. Setting guidelines around the typical accepted values for these two plotted parameters (PCR efficiency of 90 to 110% and ΔCq of 3 or greater) created a graphical box, highlighting where successful qPCR experiments (dots) should fall. While this simple dot plot was informative on its own, it wasn't sufficient to capture all of the relevant details of each qPCR experiment. In order to represent additional information, such as the linearity of the dynamic range (R^2), the overall quality of the qPCR data was scored on a scale of 1 to 5, with 5 representing the highest quality. This scoring method was built upon previous work by Hall et al.[3]. Additional performance criteria captured using the 5-point quality score included precision (reproducibility), fluorescence signal consistency, curve steepness, and sigmoidal curve shape. Parameters for these five criteria were established to identify when the quality score should be penalized. Scoring criteria differed slightly for probe-based chemistry compared to intercalating dye-based detection (Table 1) due to differences in typical curve shape.

Once assigned, the quality score for each amplicon was represented by the dot size and opacity. The higher the quality score, the larger the dot. Additionally, quality scores of 4 and 5 were represented as solid dots while a score of 3 or less was captured as an open circle for simple visual screening of performance. Amplicons falling in the box and receiving a quality score of 4 or 5 represented high quality, reliable qPCR data. The dots in boxes method allowed multiple targets and conditions to be plotted on a single graph and compared quickly, creating an efficient, high-throughput visual method for data analysis.

To rigorously test qPCR performance, experiments were designed to

	Intercalating Dye Chemistry	Hydrolysis Probe Chemistry
Linearity	$R^2 \geq 0.98$	$R^2 \geq 0.98$
Reproducibility	Replicate curves shall not vary by more than 1 Cq*	Replicate curves shall not vary by more than 1 Cq*
RFU Consistency	Maximum plateau fluorescence signal for all curves shall be within 20% of the mean. Fluorescence signal shall not be jagged.	Increase of fluorescence signal shall be consistent for all curves, exhibiting parallel slopes. Fluorescence signal shall not be jagged.
Curve Steepness	Curves shall rise from baseline to plateau within 10 Cq values or less.	Curves shall rise from baseline to 50% maximum RFU within 10 Cq values or less.
Curve Shape	Curves shall exhibit a sigmoidal shape, resulting in a plateau of fluorescence signal.	Curves need not be sigmoidal, but shall appear to be reaching a horizontal asymptote by the last PCR cycle.

Table 1. Criteria for developing quality score metrics for dots in boxes analysis

NEW ENGLAND BioLabs® Inc.

simultaneously evaluate efficiency over a broad dynamic range of input concentrations; sensitivity by assessing low-input detection; and specificity by assessing off-target amplification. To accomplish this, qPCR efficiency was measured over a five-log dilution of template with data collected in triplicate for each dilution and a NTC. For genomic targets, an average of ~2 copies per reaction was routinely tested to assess the limits of low input detection. Since the ΔCq incorporates both the Cq of the lowest input and that of the NTC [ΔCq = Cq(NTC) – Cq(lowest input)], it allows sensitivity and specificity to be captured in a single variable. Inability to amplify the lowest template dilution results in a ΔCq of 0 in most cases, since curves failing to cross the threshold are automatically given a Cq value corresponding to the total number of amplification cycles. The presence of non-specific or contaminating amplification in NTC reactions also reduces the ΔCq, such that either lack of low-input amplification or excessive off-target amplification can push the ΔCq below the passing (≥3) threshold. Target specificity was also evaluated using denaturation or melt curves for all intercalating dye-based qPCR assays, although this information was not captured in the dot plot.

Conclusion

Dots in boxes is a powerful, high-throughput data analysis method based on the MIQE guidelines. It enables rapid, concise comparison of qPCR performance across many targets and for multiple reagents, conditions and/or protocols, permitting an overview of qPCR performance over thousands of reactions where such visualization was not previously possible. Combining the dots in boxes analysis method, a range of target test panels, and a custom LIMS enabled us to create and mine large data sets for information, identify critical variables that affect amplification in qPCR, and harness this information to optimize qPCR reagents. The dots in boxes analysis tool was thus invaluable in development of the Luna qPCR and RT-qPCR reagents, and will continue to benefit future qPCR evaluation and development efforts.

Description	Rxn Size	Cat. No.	Unit
Luna Universal qPCR Master Mix	200	**103307-260**	**Each**
Luna Universal qPCR Master Mix	500	**103307-258**	**Each**
Luna Universal Probe qPCR Master Mix	200	**103307-264**	**Each**
Luna Universal Probe qPCR Master Mix	500	**103307-262**	**Each**
Luna Universal One-step RT-qPCR Kit	200	**103307-250**	**Each**
Luna Universal One-step RT-qPCR Kit	500	**103307-248**	**Each**
Luna Universal Probe One-step RT-qPCR Kit	200	**103307-254**	**Each**
Luna Universal Probe One-step RT-qPCR Kit	500	**103307-252**	**Each**

qTOWER³ and qTOWER³ *touch*

analytikjena
An Endress+Hauser Company

qPCR Thermal Cyclers

- Homogenous (±0.15°C) 96-well qPCR for up to six targets
- Rapid heating/cooling rates of 8.0°C/sec and 6.0°C/sec, respectively
- Completely calibration- and maintenance-free for the life of the system
- 10-year optical system warranty; two-year warranty on remainder of system (free upgrade to three years upon registration)

All qTOWER³ models include the qTOWER³ system, Analytik Jena's PC-based qPCRsoft software to conduct qPCR and perform analysis, 115V power cable, USB cable, and user manual.

Description	Cat. No.	Unit
qTOWER³ Real-Time PCR	75830-232	Each
qTOWER³ G Real-Time PCR	75830-234	Each
qTOWER³ *touch* Real-Time	75830-236	Each
qTOWER³ G *touch* Real-Time PCR	75830-238	Each

VWR COLLECTION designed for reliability

VWR® Basic Air Jacketed CO_2 Incubator

- 5.3 cu. ft. stainless steel internal chamber volume with three standard shelves
- On-demand 90°C moist heat decontamination cycle for simplified cleaning
- Fan-assisted airflow and in-chamber sensors maintain a uniform and stable growth environment
- Dual temperature probes for over-temperature protection and TC CO_2 sensor for long lasting, reliable performance
- Integrated pan design for fast recovery and high relative humidity
- Three-year part and labor warranty

Value and performance for everyday cell culture applications, this unit offers a reliable growth environment with the added convenience of on-demand high heat decontamination.

Volume, L (cu. ft).	Cat. No.	Unit
150 (5.3)	10810-888	Each

VWR bioMarke™

VWR Literature Library
C/O Archway
20770 Westwood Drive
Strongsville, OH 44149

PRSRT STD
US POSTAGE
PAID
PERMIT 293
MIDLAND MI

ATTN: POST OFFICE: Electronic Service Requested

VWR We Enable Science 1.800.932.5000 vwr.com

0817 25M Lit. No. 930089

ATTN: MAILROOM: If addressee is no longer with the organization, please deliver to laboratory products buyer. Thank you.

ENVIRO/TECH INK
Enviro/Tech is a registered trademark.

FSC www.fsc.org MIX Paper from responsible sources FSC® C084269

VWR We Enable Science

IgGy Antibody Selector. . .

Search | Select | Simple

Using the IgGy Antibody Selector makes searching for antibodies easier. VWR has brought together a multitude of antibody suppliers and manufacturers with hundreds of thousands of antibodies to meet your specific application needs.

With VWR, IgGy offers:

- More than 350,000 antibodies
- Brands you know and trust
- Wide range of conjugations
- Choices from multiple suppliers
- Resource for all application areas

vwr.com/antibody